

1-1-2013

Efficient Generation of Power In Medium Voltage Direct Current Systems: Variable Speed Operation and Rectifier Considerations

DAN LI

University of South Carolina - Columbia

Follow this and additional works at: <http://scholarcommons.sc.edu/etd>

Recommended Citation

LI, D. (2013). *Efficient Generation of Power In Medium Voltage Direct Current Systems: Variable Speed Operation and Rectifier Considerations*. (Doctoral dissertation). Retrieved from <http://scholarcommons.sc.edu/etd/2469>

This Open Access Dissertation is brought to you for free and open access by Scholar Commons. It has been accepted for inclusion in Theses and Dissertations by an authorized administrator of Scholar Commons. For more information, please contact SCHOLARC@mailbox.sc.edu.

EFFICIENT GENERATION OF POWER IN MEDIUM VOLTAGE DIRECT CURRENT
SYSTEMS: VARIABLE SPEED OPERATION AND RECTIFIER CONSIDERATIONS

by

Dan Li

Bachelor of Engineering
Shanghai Maritime University, 2006

Master of Science
Mississippi State University, 2009

Submitted in Partial Fulfillment of the Requirements

For the Degree of Doctor of Philosophy in

Electrical Engineering

College of Engineering and Computing

University of South Carolina

2013

Accepted by:

Roger A. Dougal, Major Professor

Herbert L. Ginn III, Committee Member

Charles Brice, Committee Member

Jamil Khan, Committee Member

Abdelhamid Ouroua, Committee Member

Lacy Ford, Vice Provost and Dean of Graduate Studies

© Copyright by Dan Li, 2013
All Rights Reserved.

DEDICATION

To my Lord Jesus Christ,

who gave me the opportunity to pursue Ph.D. in Electrical Engineering.

To my parents, Taishan Li and Shujin Wang,

who have never attended universities, but have always valued education.

To my siblings: Lydia, Grace, and Darris,

who have always taken accountability and shown your love to me.

To my brother in law, Hui and nephew Jeremy,

who have been a blessing for me since joining in the family.

ACKNOWLEDGEMENTS

To my advisor, Dr. Roger A. Dougal: You are a big thinker, who makes the best use of every moment and opportunity! Thanks for encouraging me to think big, broadening my mind, and being there for me whenever I need your guidance. As an engineer, a scientist, and a professor, you are a person with strong ethics, and I thank you for passing these values to me.

To my co-advisor, Dr. Herbert L Ginn III, what can I say? Thanks for your advisement and challenging me to rethink my ideas since my master's program at Mississippi State University in 2007. I appreciate your sending me to USC, and even continuously guiding me through this Ph.D. program. To Mrs. Ginn, Sufang, thank you for always thinking about me and making my whole stay in the United States more enjoyable.

To Dr. Abdelhamid Ouroua with the University of Texas at Austin, thanks for countless discussions in spite of distance, which cleared many of my thoughts in the process of this work. To Dr. Charles Brice and Dr. Jamil Khan, thank you for invaluable feedback which helped me develop this work.

To Dr. Chuck Kwok and Mrs. Shirley Kwok, without your hospitality and support over the years in Columbia, I would not have been able to finish this Ph.D.

To EE staff members and colleague students: Hope Johnson, Rich Smart, Nat Paterson, Rostan Rodrigues, Ugo Ghisla, Huaxi Zheng, thank you for your time and efforts to make this work possible.

Last and but not least, to my Lord Jesus Christ, You have blessed me with so many kind people helping and supporting me on the journey of Ph.D. program.

ABSTRACT

By investigating variable speed operation of an engine and different types of ac-dc rectifier topologies, this dissertation provides procedures to develop and implement efficient Medium Voltage Direct Current (MVDC) power systems. The research reported here offered solutions to the following issues:

- 1) Efficiency improvement of a gas turbine by running it in variable speed operation mode.
- 2) The advantages and disadvantages of different ac-dc rectifier topologies considering both the efficiency and rectifier performance (dc bus voltage regulation, weight/size/volume of passive components, number of semiconductor devices, displacement power factor, complexity of control strategy, etc.)
- 3) Implementation of variable speed MVDC power system if variable speed operation brings great advantages for fuel saving.

A semi-theoretical analysis was developed to address issue 1). This analysis revealed the optimal efficiency and the corresponding optimal speed as a function of shaft load for both single-shaft and twin-shaft gas turbines. These semi-theoretical results were confirmed by detailed simulations that show it is possible to achieve as much as 15% reduction in fuel consumption when variable speed operation is used instead of fixed

speed, for a generating plant to electrically propel a ship having powering characteristics similar to those of a DDG-51.

A series of boost type rectifiers for applications in MVDC power systems were compared to address issues 2). The comparison included only boost rectifiers since higher distribution voltage leads to higher efficiency. The boost type rectifiers are diode rectifier with boost chopper (diode rectifier), three-level diode clamped voltage source converter (VSC), and modular multilevel converter (MMC). The comparison metrics include complexity of control strategy, number of switching devices, number/value/weight/volume of inductors and capacitors, the dc bus voltage performance (peak-peak voltage ripple, overshoot, and settling time), the total harmonic distortion (THD) of the ac side input current and voltage, displacement power factor (DPF), power efficiency for different load conditions, and performance under variable ac frequency operation. The comparison shows that MMC is the most efficient and provides the best dc bus performance, by adding more capacitors (both number of capacitors and total weight), and more complex control schemes into the system. VSC provides a relative high efficiency and dc bus performance with less passive components, which indicates VSC is a good choice considering both performance and cost.

A procedure to implement an integrated variable speed MVDC power system was proposed to address issues 3). For each component of dc power generation chains, gas turbine, synchronous generator, and ac-dc rectifier, their steady-state efficiencies and system efficiency vs. dc load were analyzed. The relative system efficiency improvement (an index of fuel reduction) can be up to 35% for 10% loading. The relative efficiency improvement decreases to 5% as the dc load increases to 45% loading. Following the

procedure, a variable speed MVDC power system simulation model was developed. The dynamic response shows that the system can track the speed command for different load demands while yielding the highest efficiency and good system stability.

TABLE OF CONTENTS

DEDICATION.....	iii
ACKNOWLEDGEMENTS.....	iv
ABSTRACT.....	vi
LIST OF TABLES	xi
LIST OF FIGURES	xii
LIST OF SYMBOLS	xv
CHAPTER 1 INTRODUCTION	1
1.1 CONTRIBUTIONS OF DISSERTATION	1
1.2 MOTIVATION	3
1.3 PROBLEM OF DESCRIPTION.....	6
1.4 APPLIED SOLUTION	6
1.5 STATE OF ART	8
CHAPTER 2 FUEL EFFICIENCY OPTIMIZATION IN GAS TURBINE.....	11
2.1 NOMENCLATURE	11
2.2 PROBLEM STATEMENT AND SOLUTION APPROACH.....	12
2.3 BACKGROUND/LITERATURE REVIEW	14
2.4 SEMI-THEORETICAL ANALYSIS	16
2.5 MODELING AND SIMULATION.....	22
2.6 TEST ON GIVEN LOAD PROFILE	30
2.7 TORQUE CHARACTERISTIC COMPARISON	33

2.8 DISCUSSION AND CHAPTER SUMMARY	34
CHAPTER 3 COMPARISON OF POSSIBLE RECTIFIERS TOPOLOGIES IN MVDC POWER SYSTEMS	35
3.1 PROBLEM STATEMENT	35
3.2 COMPARISON FACTORS	37
3.3 RECTIFIER OF TOPOLOGIES AND PARAMETERS	38
3.4 RESULTS AND MERITS COMPARISON	43
3.5 VARIABLE SPEED OPERATION	53
3.6 MERITS COMPARISON SUMMARY	54
3.7 DISCUSSION AND CHAPTER SUMMARY	57
CHAPTER 4 INTEGRATED MVDC POWER SYSTEM IN VARIABLE SPEED OPERATION MODE	59
4.1 PROBLEM DESCRIPTION AND BACKGROUND	59
4.2 APPROACHES AND ANALYSIS RESULTS	63
4.3 RESULTS	67
4.4 TEST ON GIVEN LOAD PROFILE	71
4.5 DISCUSSION AND CHAPTER SUMMARY	73
CHAPTER 5 CONCLUSION AND FUTURE WORK	75
5.1 CONCLUSION	75
5.2 FUTURE WORK	76
REFERENCES	77
APPENDIX A GAS TURBINE	84

LIST OF TABLES

Table 2.1 Nomenclature of Chapter 2.....	11
Table 2.2 Example of 1- day fuel consumption for constant and variable speed operation of gas turbine	32
Table 3.1 Recommended MVDC voltage classes in ship system [46].....	36
Table 3.2 Data of test system.....	38
Table 3.3 Recommended requirements of voltage variations for dc system [47]	39
Table 3.4 Number of semi-conductor devices in rectifiers.....	43
Table 3.5 Filters components comparison	44
Table 3.6 DC bus voltage performance	51
Table 3.7 THD of phase voltage and current.....	52
Table 3.8 Merits comparison summary	55
Table 4.1 Data of test system.....	64
Table 4.2 Example of 1- day fuel consumption for constant and variable speed operation of MVDC power systems	73

LIST OF FIGURES

Figure 1.1 Compared merits of ac-dc rectifiers	2
Figure 1.2 Power flow train of dc system	6
Figure 1.3 impact of GT efficiency on dc system efficiency.....	7
Figure 1.4 Possible applications of variable speed operation of gas turbine	10
Figure 2.1 Typical SFC vs. output shaft power for a simple-cycle GT	13
Figure 2.2 Diagram of a single-shaft GT	14
Figure 2.3 Diagram of a twin-shaft GT	15
Figure 2.4 flow chart of the approach to solve GT governing equations	20
Figure 2.5 Semi-theoretical analysis of VSO on single-shaft GT efficiency	21
Figure 2.6 Semi-theoretical results of the impact of VSO on twin-shaft GT efficiency ..	22
Figure 2.7 Single-shaft gas turbine as modeled in GasTurb.....	23
Figure 2.8 Impact of VSO on single-shaft GT efficiency (semi-theoretical and simulation)	24
Figure 2.9 Relative efficiency improvement of single-shaft gas turbine at variable speed	25
Figure 2.10 Compressor operating at speed $N=0.83$ p.u. in single-shaft gas turbine speed	26
Figure 2.11 Turbine operating at speed $N=0.83$ p.u. in single-shaft gas turbine.....	27
Figure 2.12 Compressor part load efficiency at fixed speed and variable speeds.	28
Figure 2.13 Impact of variable speed operation of twin-shaft gas turbine efficiency	29
Figure 2.14 Free power turbine speed curves [14]	30
Figure 2.15 Typical propulsion speed profile of DDG-51 [13].....	31
Figure 2.16 Variation of propulsion load power with ship speed.....	31

Figure 2.17 Torque characteristics of single-shaft GT	33
Figure 2.18 Torque characteristics of gas generator for a twin-shaft gas turbine.....	34
Figure 3.1 Diode rectifier with single-switch boost chopper.....	40
Figure 3.2 Diode rectifier with boost chopper control structure.....	40
Figure 3.3 Three-level diode clamped VSC with LCL filter	41
Figure 3.4 Control structure of three-level diode clamped VSC	41
Figure 3.5 MMC	42
Figure 3.6 Control structure of MMC.....	43
Figure 3.7 Typical V_{ce} and I_c characteristic of IGBT [58].....	46
Figure 3.8 Typical V_f and I_f characteristic of diode [58].....	47
Figure 3.9 Curve fitting of V_{ce} as a function of I_c	47
Figure 3.10 Curve fitting of V_f as a function of I_f	48
Figure 3.11 Efficiency of rectifiers at fixed speed.....	49
Figure 3.12 Waveforms of dc bus voltage	51
Figure 3.13 DPF of rectifiers	52
Figure 3.14 Phase current of diode rectifier in fixed frequency operation and variable speed operation	53
Figure 3.15 Efficiency of diode rectifier, VSC, and MMC in fixed frequency operation and variable speed operation	54
Figure 3.16 Total inductor volume comparison.....	56
Figure 3.17 Total capacitor weight comparison	57
Figure 4.1 Diagram of a MVDC power system.....	60
Figure 4.2 Power flow chart of synchronous generator.....	62
Figure 4.3 Typical efficiency curve of a synchronous generator at fixed speed	62
Figure 4.4 Efficiency of synchronous generator vs. electric load at different speeds	63
Figure 4.5 Control diagram of MVDC power system	64

Figure 4.6 Flow chart of obtaining generator efficiency at any load and speed based on a series of efficiency curves.	65
Figure 4.7 Efficiency of rectifiers vs. dc load.....	66
Figure 4.8 Flow chart of obtaining optimal speed reference of MVDC Power System... ..	67
Figure 4.9 Efficiencies and optimal speed at integrated variable speed MVDC power system	68
Figure 4.10 Relative efficiency improvement of dc system vs. dc load in VSO mode	69
Figure 4.11 Optimal speed of variable speed MVDC Power System.....	69
Figure 4.12 Phase-a voltage of generator	70
Figure 4.13 Phase-a current of generator	70
Figure 4.14 DC bus voltage	71
Figure 4.15 Typical propulsion speed profile of DDG-51 [13].....	72
Figure 4.16 Variation of propulsion load power with ship speed.....	72

LIST OF SYMBOLS

\dot{m}	mass flow rate (kg/s).
h	enthalpy (J/kg)
T_{in}	inlet temperature (K)
T_{out}	outlet temperature (K)
τ	torque (Nm)
N	speed (RPM)
ω	speed (rad/s)
$\%N$	relative speed to design speed in map
β	beta-auxiliary coordinate useful for representing table format of maps
P	pressure (Pa)
PL	pressure loss percentage
PR	pressure ratio
PR	pressure loss percentage
L	load of gas turbine in p.u.
γ	ratio of specific heat
PL	pressure loss percentage
P_o	ambient pressure
T_o	ambient temperature
HV	heating value of fuel (J.kg)
θ	temperature correction factor

P_{cond_T}	conduction loss of IGBT
P_{cond_D}	conduction loss of diode
P_R	resistance loss
v_{ce}	collector-emitter voltage of IGBT
i_c	collector current
v_f	diode forward voltage
i_f	diode forward current
v_R	voltage across the resistor
i_R	current across the resistor
t_0	moment at that calculation starts (when calculating loss of rectifier)
T	cycle of calculating loss (rectifier)
W_{on}	turn on loss of IGBT
W_{off}	turn off loss of IGBT
W_{rec}	reverse recover loss of diode
P_{dc}	dc bus load power
P_{lossT}	total loss of a rectifier caused by semi-conductors and filters
Subscripts	
C	compressor
T	turbine
$C \text{ or } T$	compressor or turbine
HT	high pressure turbine (gas generator)
LT	low pressure turbine (free power turbine)
l	load

<i>in</i>	inlet
<i>out</i>	outlet
<i>f</i>	fuel
<i>cb</i>	combustor
<i>isen.</i>	isentropic process
<i>opt_gt</i>	gas turbine in variable speed operation
<i>sg</i>	synchronous generator
<i>rect</i>	rectifier

LIST OF ABBREVIATIONS

Diode Rectifier	Diode Rectifier with Boost Chopper
DPF	Displacement Power Factor
DC	Direct Current
GT	Gas Turbine
MMC	Modular Multi-level Converter
MVDC	Medium Voltage Direct Current
PSC-PWM	Phase-shifted Carrier-based PWM
PV	Photovoltaic
SG	Synchronous Generator
THD	Total Harmonic Distortion
VSC	Three-level Diode Clamped Voltage Source Converter
VSO	Variable Speed Operation

CHAPTER 1

INTRODUCTION

1.1 CONTRIBUTIONS OF DISSERTATION

- Developed procedures to investigate gas turbine (GT) in variable speed operation (VSO)
 - Obtained the GT optimal efficiency and its corresponding optimal speed as a function of its shaft load
 - Conducted semi-theoretical analysis
 - Validated by modeling and simulation
 - Considered single-shaft (1-shaft) GT and twin-shaft (2-shaft) GT
 - The percentage of fuel saving increasing as load decreasing
 - Efficiency improvement larger for 1-shaft GT than for 2-shaft GT
 - Up to 15% fuel saving for reference mission profile DDG-51 like hull
 - Better torque-speed characteristic of 1-shaft GT by VSO
- Provided guidelines for selection of ac-dc rectifiers for MVDC power systems.
 - Boost type ac-dc rectifiers for use in MVDC systems: diode rectifier with boost chopper (diode rectifier), three-level diode clamped voltage source converter (VSC), and modular multilevel converter (MMC).

- Compared merits described as Figure 1.1, including system level, dc side factors, ac side factors, complexity and cost of rectifiers, and the impact of VSO on rectifier performance.

<p><u>System level</u></p> <ul style="list-style-type: none"> ✓ Rectifier efficiency (at rated load and part-load) <p><u>dc side factors</u></p> <ul style="list-style-type: none"> ✓ Voltage regulation (dc bus): ripple, settling time, overshoot <p><u>ac side factors</u></p> <ul style="list-style-type: none"> ✓ Voltage and current total harmonic distortion (THD) ✓ Displacement power factor (DPF) ✓ Voltage variation (ac bus: magnitude, phase angle, and frequency) <p><u>Complexity and Cost of Rectifiers</u></p> <ul style="list-style-type: none"> ✓ Complexity of rectifier control ✓ Number of switching devices ✓ Number/value/weight of inductor & capacitors <p><u>Impact of variable speed operation:</u> efficiency , ac/dc side</p>	<p>dc system: not considered</p>
--	--------------------------------------

Figure 1.1 Compared merits of ac-dc rectifiers

- System level (efficiency): MMC is the most efficient and it remains efficient almost independent of load conditions, while the efficiencies of VSC and diode rectifier decreases as the load decreases.
- DC side factors: MMC has the best dc performance, including low overshoot, and low ripple. MMC has only 3.2% voltage overshoot compared to diode rectifier's 18.3% and VSC's 26.5% following a 75% load shed.
- AC side factors: MMC has the best ac side performance, with only 0.8% THD of voltage and current, independent of loading conditions.

- All of the studied rectifiers can achieve unity displacement power factor (DPF) under rated conditions.
- The DPF of the diode rectifier decreases as the load decreases, falling to as low as 0.61 at 25% loading.
- The performances of VSC and MMC are relatively independent of speed while variable frequency operation increases the DPF of a diode rectifier to 0.71 from 0.61 under 25% loading.
- Although the MMC has more components, it actually needs fewer switching devices as compared to device series connections present in diode rectifier and VSC.
- The MMC's capacitor weight is about 6 times that of VSC and about 8 times that of diode rectifier. But the MMC's inductor is negligible compared to that of diode rectifier and VSC.
- The investigation of integrated MVDC power system with variable speed operation shows that the dc system efficiency could be improved up to 35% at 10% loading compared to fixed speed operation.
- Presented a method to implement the variable speed MVDC power system.

1.2 MOTIVATION

1.2.1 DC POWER DISTRIBUTION CONCEPT

From the perspective of energy concern, the dc power distribution is becoming a trend to displace the ac power distribution in industrial systems, marine applications, groups of

buildings, data centers, etc. As in [36], the potential benefits of the dc power distribution system are summarized below:

- With the increasing use of the equipments which operate on dc voltage, the dc power distribution system eliminates the corresponding ac-dc conversion which is required in ac power distribution system.
- Because of improved inverters, dc power is more efficiently and easily converted to the ac power.
- The dc power delivery may enhance micro-grid system integration, operation, and performance. In dc power distribution system, the solid-state switching can quickly interrupt faults.
- In the dc power distribution system, the distributed generation devices or energy storages (other than flywheels) are able to be connected to the system without dc-ac conversion, since those Distributed generation sources or energy storages devices are dc voltage, such as photovoltaic (PV), fuel cells, batteries, etc.
- The dc power delivery concept is greatly preferable in facilities such as data centers. As in [37], compared to ac system, dc power can improve the system efficiency up to 7% in data centers.
- For marine applications, dc power distribution is even more preferable in terms of equipment weight saving because of the elimination of bulky transformers and main ac switch gears.

- The dc power distribution system concept enables the decoupling the engine speed from the generated terminal voltage, which makes the concept of running the engine at variable speed feasible.
- Generally, the dc system has a higher power density compared to ac system for a given generator, because in a dc power generation module speed reduction gears are not needed and both the generator and the ac-dc converter can share the supporting systems including cooling and noise isolation features, elimination of cabinetry and bus cables [37].
- The controlled-converter in a dc power system enables the use of permanent magnet synchronous generators without adding extra component, by regulating dc bus voltage to a desired value. Permanent magnet synchronous generator in dc power systems greatly reduces the weight and volume of the synchronous generator and the ohmic loss of the rotor resulting in less cooling demand.

Overall, the concept of dc power distribution system has great potential benefits in terms of efficiency and ease of integration of future distribution technologies. In addition, with the concept of running the engine and generator at variable speed, the system efficiency will improve even more if the turbo-generators run at optimal operating speeds for a given set of load.

1.2.2 VARIABLE SPEED OPERATION OF GAS TURBINE GENERATOR SET

The dc power system makes it feasible that the gas turbine generator set runs at variable speed operation, which improves the part-load efficiency of gas turbine.

1.3 PROBLEM OF DESCRIPTION

The objective of this dissertation is to develop a procedure to improve the part-load efficiency in the directly-coupled gas turbine generator dc power system topology by adjusting the engine speed to the power demand and considering different ac-dc rectifiers. In details, this dissertation answered three questions:

- Feasibility of VSO improving a GT part-load efficiency?
 - Efficiency gain
 - Speed range
- Recommendation of ac-dc rectifier topologies in MVDC power systems? Especially, the impact of VSO on the rectifier performance
- The way to implement a variable speed MVDC power system?

1.4 APPLIED SOLUTION

Considering the power flow train of a dc system as in Figure 1.2, the dc system efficiency depends on the gas turbine efficiency, synchronous generator (SG) efficiency, and ac-dc rectifier efficiency.

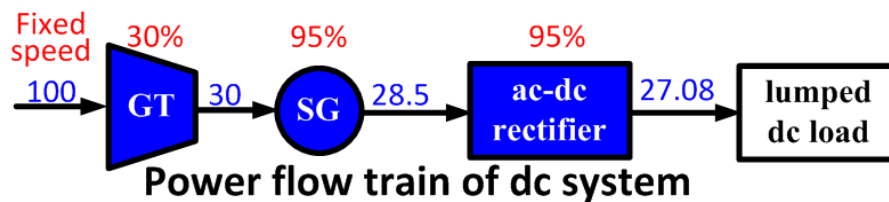


Figure 1.2 Power flow train of dc system

The first step of solving the described problem in the previous section is to decide the efficiency improvement priority of the dc system. In this work, gas turbine efficiency improvement was considered the first priority in terms of dc system efficiency improvement for the following reasons:

- a. Gas turbine is the least efficient among the three components (GT, SG, and ac-dc rectifier). For a simple cycle gas turbine, its efficiency is less than 35%, while for synchronous generator and ac-dc rectifier; their efficiencies are more than 95%, or even up to 98%. To illustrate that dc system efficiency improvement is dependent on gas turbine efficiency improvement; Figure 1.3 shows different combinations of gas turbine efficiency, synchronous generator efficiency, and ac-dc rectifier efficiency. The first row of the table is the reference case when the system runs at fixed speed. By increasing gas turbine efficiency 1% and decreasing SG efficiency and ac-dc rectifier efficiency 1%, it gives total dc system efficiency 27.39%. By decreasing gas turbine efficiency 1%, and increasing SG and ac-dc rectifier efficiency 1%, it gives total dc system efficiency 26.73%. Figure 1.3 indicates that improving gas turbine efficiency is the key to improve dc system efficiency.

Efficiency (%)			
GT	SG	ac-dc rectifier	Total
30	95	95	27.08
31↑	94↓	94↓	27.39↑
29↓	96↑	96↑	26.73↓

fixed speed (reference) →

Following the trend of GT efficiency

Figure 1.3 impact of GT efficiency on dc system efficiency

- b. The part-load efficiency of the gas turbine decreases much more dramatically compared to synchronous generator and ac-dc rectifier, as seen in Figure 2.1 and the following secretions.
- c. With gas turbine efficiency improvement as first priority, the control of implementation of such system is less challenged compared to the case of considering all the three components' efficiency improvement (GT, SG, and ac-dc rectifier) equally important.

The second step of the solution is the investigation of gas turbine variable speed operation which is presented in Chapter 2. The third step of the applied solution is about recommendation of ac-dc rectifier solutions in MVDC power systems as described in Chapter 3. The last step of the solution is the applied method to implement the variable speed MVDC power system illustrated in Chapter 4.

1.5 STATE OF ART

For variable speed operation of gas turbine, there are two representative references. One is about semi-theoretical analysis by N. Zhang, and R. Cai [4]; and the other one is about gas turbine modeling and simulation by W. I. Rowen [9]. Ref [4] illustrated their work for the mechanical engineering audience without details of procedures. Compared to Ref [4], this dissertation improved

- presented details of procedures, especially easily understandable by electrical engineers.

Gas turbine and generator have two ways for connecting their respective shafts, one is through a gear box; the other is through direct coupling. The gearbox needs internal inspection and long-time overhaul examination which momentarily reduce power generation capacity. Furthermore, in a gas turbine power system, the gear box is one of the most important factors of decreasing overall efficiency. Roughly, the gearbox loss will be 2% of the total output power of gas turbine [71]. Direct coupling eliminates the gear box for weight and volume reduction, as well as efficiency improvement.

Without gearbox, variable speed operation (VSO) has three possible applications as shown in Figure 1.4. In fixed frequency ac power system: ac-ac conversion is required to match generator frequency to fixed system frequency. Another application of VSO is in variable frequency ac power systems, which allows power system frequency to vary and eliminates the inefficiency of the converters. The feasibility of VSO in variable frequency ac power system depends on the line loads, and the speed range. The third application of VSO is in dc power systems, the rectifier decouples the engine speed from the dc bus distribution voltage. The total dc system efficiency depends on the efficiency of gas turbine, synchronous generator, and ac-dc rectifier. This dissertation is focused on the third application of VSO, in dc power systems.

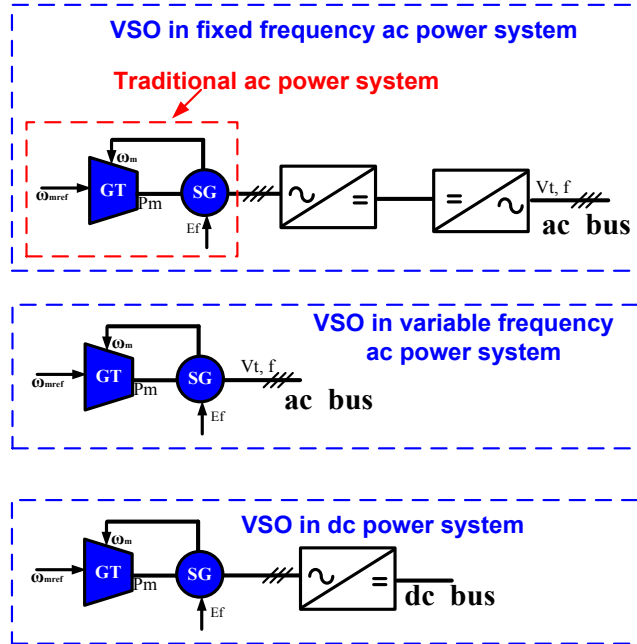


Figure 1.4 Possible applications of variable speed operation of gas turbine

There is no literature about efficient generator of power in MVDC systems by VSO of GT.

Ref [5] with E.ON Energy Research Center at Aachen, Germany, investigated VSO in fixed frequency ac power system with permanent magnet synchronous generator connected to a diode rectifier and a three level neutral-point-clamped inverter. The results of ref [5] shows VSO increased the 10 MVA system efficiency by 2.5% at 40% load.

This dissertation covers variable speed operation in MVDC system and comparisons of possible ac-dc rectifiers.

CHAPTER 2

FUEL EFFICIENCY OPTIMIZATION IN GAS TURBINE

2.1 NOMENCLATURE

Table 2.1 Nomenclature of Chapter 2

Variable	Meaning
\dot{m}	mass flow rate (kg/s)
h	enthalpy (J/kg)
T_{in}	inlet temperature (K)
T_{out}	outlet temperature (K)
τ	torque (Nm)
N	speed (RPM)
ω	speed (rad/s)
$\%N$	relative speed to design speed in map
η	efficiency
β	beta-auxiliary coordinate useful for representing table format of maps
P	pressure (Pa)
PL	pressure loss percentage
PR	pressure ratio
L	load of gas turbine in p.u.
γ	ratio of specific heat
P_o	ambient pressure
T_o	ambient temperature
HV	heating value of fuel (J/kg)
θ	temperature correction factor $\theta = \frac{T_o}{288.15 K}$

δ	pressure correction factor $\delta = \frac{P_o}{101.325 \text{ kPa}}$
Subscripts	
C	compressor
T	turbine
$C \text{ or } T$	compressor or turbine
HT	high pressure turbine (gas generator)
LT	low pressure turbine (free power turbine)
l	load
in	inlet
out	outlet
f	fuel
cb	combustor
$isen.$	isentropic process

2.2 PROBLEM STATEMENT AND SOLUTION APPROACH

For electrical power generation, the output shaft of gas turbine typically runs at a fixed speed, the design speed that matches the generator speed to the frequency of the ac distribution system, typically 50 or 60Hz. Despite the previously mentioned advantages of gas turbines, the well-known disadvantage is their low efficiency when operating at part-load [4] [5]. Figure 2.1 shows a typical variation of specific fuel consumption (SFC) with turbine output power in p.u., indicating SFC is poor at low output power. For this particular curve, when the load is 20% of rated power, the specific fuel consumption is about 1.9 times the rated SFC. This fast deterioration of efficiency at part load is an inherent problem for gas turbines

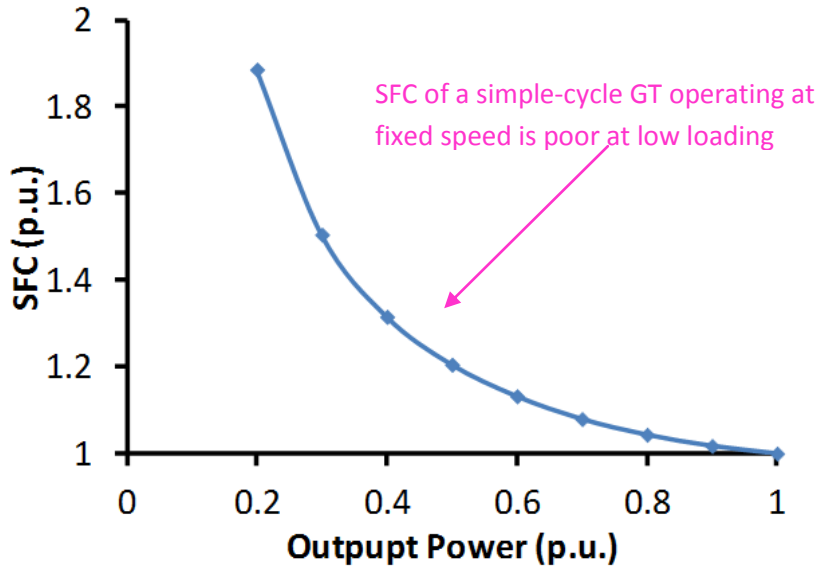


Figure 2.1 Typical SFC vs. output shaft power for a simple-cycle GT

However variable speed operation is emerging as a viable method to improve part-load efficiency, where it has been explored for fuel cell gas turbine hybrid systems [33] [34]. For power generation using turbogenerators, variable speed operation can be realized for both ac and dc systems. In dc systems, a controlled rectifier can maintain the desired dc bus voltage as the speed varies. In ac systems, the desired ac bus voltage can be achieved by the combination of an ac-dc rectifier (either controlled or uncontrolled) with a dc-ac inverter. Of course excitation field control can also be applied in both cases, except in the case of permanent magnet machines. Ref [5] described the part-load efficiency improvement possible for a gearless medium voltage variable speed gas turbine ac system where the desired ac bus voltage was controlled by the inverter only and the rectifier was an uncontrolled diode bridge. That work did not describe modeling of gas turbines, which is critical to understanding and quantifying the variable speed operating mode. A general discussion on this topic is provided in the next paragraph.

2.3 BACKGROUND/LITERATURE REVIEW

2.3.1 GAS TURBINE OVERVIEW

Gas turbines are widely used in both mechanical drive applications and electrical power generation as prime movers for their advantages in weight, compactness, fast response to load changes, and flexibility of fuel choices [1][2][3]. Because of these advantages, gas turbines are largely used in remote and autonomous power plants where space is at premium, by utilities as peak power sources, by the aerospace industry, and in marine applications to power the propulsion system and generate electricity. According to the configuration of the shafts of gas turbines, they are categorized as single-shaft and twin-shaft gas turbines. For single-shaft gas turbine, both the compressor and the turbine share the same shaft as shown in Figure 2.2. The twin-shaft gas turbine consists of a single-shaft gas turbine, called the gas generator (or high pressure turbine), driving a free power turbine (or low pressure turbine), as depicted in Figure 2.3. Single-shaft gas turbines and gas generator sections of twin-shaft turbines may also consist of multiple-shafts forming two or more spools and referred to as multi-spool gas turbines.

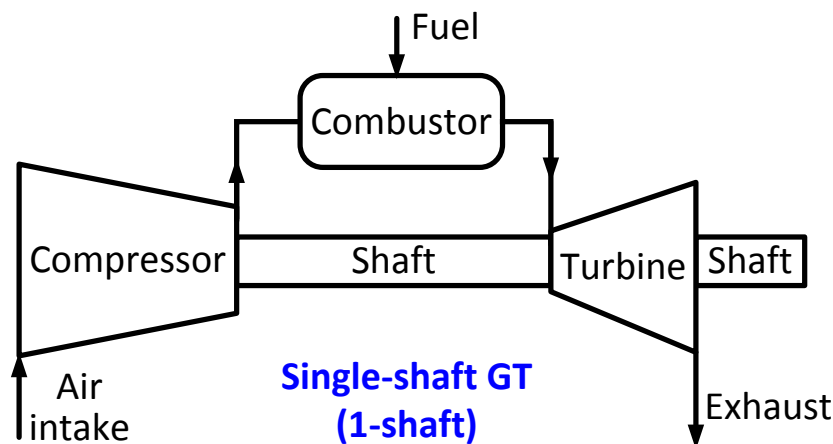


Figure 2.2 Diagram of a single-shaft GT

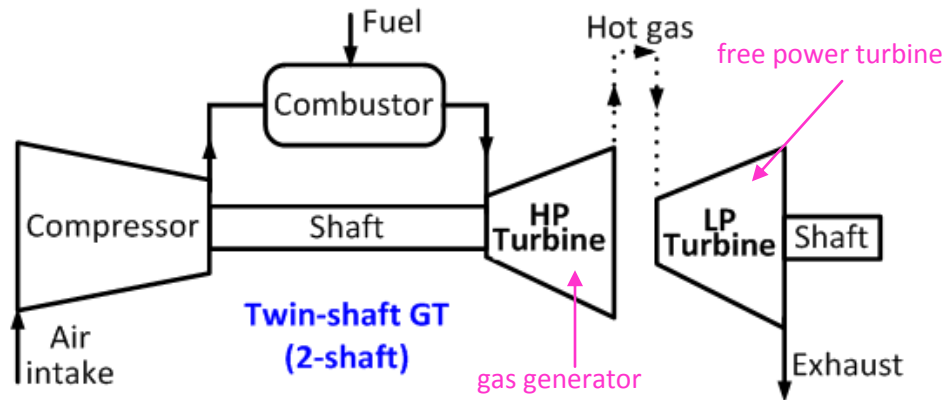


Figure 2.3 Diagram of a twin-shaft GT

2.3.2 METHODS OF GAS TURBINE MODELING

An overview of gas turbine models was given in [6] which refers to physical models [14], [16]-[21], time constant-based models[9], IEEE standard models[22][23], aero-derivative models[7], GAST model [24], WECC/GGOV1 model [25]-[28], CIGRE model [29], and frequency dependent models [30][31]. Physical models derive mathematical equations for each engine stage based on the laws of thermodynamics. Some models, [9], [22], and [23], are accurate only over a very narrow range of speeds such as those representing heavy duty gas turbines for power generation. Models of aero-derivative engines, as described in [7], have been developed for twin-shaft gas turbines, but can also be applied to the situation where the speed of the free power turbine is fairly constant. The other models are all similar to the model described in [9] in terms of control schemes, which are all limited to a fairly constant speed range too. In the area of gas turbine modeling, a lot of work [7] [8] involves design point modeling [9], which provides mathematical equations for torque, speed, and fuel flow rate near the design operating

point. The coefficients of the mathematical equations are tuned based on field measurement data from real gas turbine power plants [8] [10]. There is another approach [11] to develop gas turbine models for both design and off-design performance analysis. This approach consists of constructing artificial performance maps of compressors and turbines which are constructed from the generalized maps found in the literature [32] with appropriate scaling techniques. Similar to other techniques, it is to be validated with test measurement data from real plants because of the uncertainty in assumptions that are necessarily made to produce the artificial maps.

2.4 SEMI-THEORETICAL ANALYSIS

In this work, artificial turbine maps were used to model the gas turbine with the commercial software GasTurb [12], to evaluate its off-design performance. A semi-theoretical analysis of gas turbine off-design performance was also conducted for comparison with the modeling and simulation results. The semi-theoretical analysis includes thermodynamic equations that govern gas turbine engine operation to evaluate its off-design performance.

Gas turbine off-design performance is analyzed by using basic thermodynamic equations that govern gas turbine operation, and typical compressor and turbine characteristic maps. The characteristic maps describe relationships among pressure ratio, efficiency, mass flow rate, and rotational speed. Manufacturer's characteristic map data of a particular gas turbine component available from the literature, are scaled and used for a particular engine configuration [35]. This analysis is termed as semi-theoretical with respect to complete analytical model, since it combines both the characteristic map data, which are empirical data and the governing thermodynamic relations.

2.4.1 ASSUMPTIONS

In this semi-theoretical analysis, the thermodynamic equations are developed based on the following assumptions:

- There is no bleed, which means that mass flow consists of air intake at the compressor, fuel input at the combustor, and hot gas exhausts through the exhaust ducts only.
- Pressure losses in the compressor, turbine, and ductings are neglected.
- Mechanical losses in pumps and bearings are neglected.
- Pressure loss across the combustion chamber is a constant small percentage of the combustor inlet pressure.

$$P_{cb_out} = P_{cb_in}(1 - PL_{cb}) \quad (2.1)$$

2.4.2 COMPATIBILITIES OF COMPONENTS AND THERMODYNAMIC EQUATIONS

All off-design equilibrium running points are calculated by satisfying the compatibilities of rotational speeds, mass flow, and work among the various gas turbine components as discussed below [14].

Speed Compatibility: for a single shaft gas turbine, the compressor and turbine are directly coupled giving (2.2):

$$N_C = N_T = N_{load} \quad (2.2)$$

For a twin-shaft gas turbine, the compressor is coupled with the gas generator while the free power turbine is connected to the load. The relations are expressed as (2.3) and (2.4).

$$N_C = N_{HT} \quad (2.3)$$

$$N_{LT} = N_{load} \quad (2.4)$$

Mass Flow Compatibility: without bleed effect, mass flow at the turbine inlet is the sum of compressor outlet air mass flow and fuel mass flow at the combustor as (2.5).

$$\dot{m}_{T_{inlet}} = \dot{m}_{C_{air}} + \dot{m}_{cb_{fuel}} \quad (2.5)$$

Power Flow Compatibility: neglecting losses, the power generated by the turbine is consumed by the compressor and load as (2.6) and (2.7).

$$\dot{W}_T = \dot{W}_c + \dot{W}_l \quad (2.6)$$

$$\dot{W}_{C\ or\ T} = \dot{m} \left(h(T_{in_{C\ or\ T}}) - h(T_{out_{C\ or\ T}}) \right) \quad (2.7)$$

The enthalpy variation with temperature is available in the literature. In this work, the curve fitted correlation of enthalpy and temperature from the software GasTurb [12] to calculate the enthalpy and power therefrom, are used. The outlet temperatures of compressor and turbine are calculated as (2.8) and (2.9).

$$T_{out_{C}} = T_{in_{C}} + \frac{T_{in_{C}}}{\eta_{C,isen}} \left(PR_C^{\frac{\gamma-1}{\gamma}} - 1 \right) \quad (2.8)$$

$$T_{out_{T}} = T_{in_{T}} - T_{in_{T}} * \eta_{T,isen} \left(1 - \left(1/PR_T^{\frac{\gamma-1}{\gamma}} \right) \right) \quad (2.9)$$

The pressure ratio, mass flow, and efficiency are functions of speed, and auxiliary coordinate β [12] as (2.10) to (2.12) below. The auxiliary coordinate β prevents ambiguity between vertical and horizontal speed line characteristics representation of the map, and thus helps with data retrieval from the map table.

$$PR_{C\ or\ T} = f_1(\beta, \%N) \quad (2.10)$$

$$\left(\dot{m} \frac{\sqrt{\theta}}{\delta} \right)_{C \text{ or } T} = f_2(\beta, \%N) \quad (2.11)$$

$$(\eta_{isen})_{C \text{ or } T} = f_3(\beta, \%N) \quad (2.12)$$

where

$$PR_C = \frac{P_{out_C}}{P_{in_C}} \quad (2.13)$$

$$PR_T = \frac{P_{in_T}}{P_{out_T}} \quad (2.14)$$

With the scaling laws (2.15) to (2.17) below which help generalize the use of available component maps to different configuration [35], the pressure ratio, mass flow rate, and isentropic efficiency are given by

$$PR = \frac{PR_{des} - 1}{P_{map,des} - 1} (PR_{map} - 1) + 1 \quad (2.15)$$

$$\dot{m} = \frac{\dot{m}_{des}}{\dot{m}_{map,des}} (\dot{m}_{map}) \quad (2.16)$$

$$\eta_{isen} = \frac{\eta_{isen,des}}{\eta_{isen,map \ des}} (\eta_{isen,map}) \quad (2.17)$$

Finally, the gas turbine efficiency and torque are calculated as (2.18) and (2.19).

$$\eta_f = \frac{\dot{W}_T - \dot{W}_C}{\dot{m}_f * HV} \quad (2.18)$$

$$\tau_{C \text{ or } T} = \frac{\dot{W}_{C \text{ or } T}}{\omega} \quad (2.19)$$

An iterative approach is needed to solve the governing equations (2.2) to (2.19) and follows the procedure, for a single-shaft gas turbine, as described below [14] with its corresponding flow chart in Figure 2.4:

- Select a speed line on the compressor map.
- The corresponding point on the turbine characteristic is obtained from consideration of compatibility of rotational speed and mass flow.
- With matched compressor and turbine characteristics, check whether the generated work corresponding to the selected operating point is compatible with the required driven load.

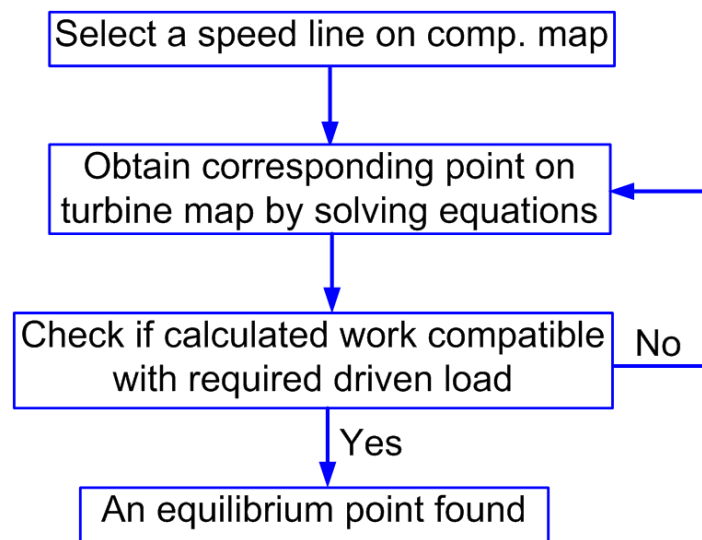


Figure 2.4 flow chart of the approach to solve GT governing equations

For twin-shaft gas turbine, the matching of gas generator and free power turbine is also needed. In this work, multivariable Newton Raphson iteration method is used to do the iterative calculations until an equilibrium running point is found.

2.4.3 SEMI-THEORETICAL RESULTS OF SINGLE-SHAFT GAS TURBINE

Using the semi-theoretical analysis method, the above equations were iteratively solved. The analysis investigated a single-shaft gas turbine (5.71 MW, 15808 RPM) with

available compressor and turbine characteristic maps. The output data were analyzed and fitted for the optimal efficiency and speed as a function of load.

$$\eta_{opt_1shaft} = 28.1L^3 - 71L^2 + 64.4L + 12.5 \quad (2.20)$$

$$N_{opt_1shaft} = 1.5L^4 - 4.2L^3 + 4L^2 - 1.4L + 1.03 \quad (2.21)$$

These results (dashed lines) are plotted on Figure 2.5 to show the impact of VSO on single-shaft gas turbines efficiency from semi-theoretical analysis. The green curve is the optimal speed corresponding to the optimal efficiency. For a given output shaft power, VSO can always bring higher efficiency by running the engine at the optimal speed other than fixed speed. The improvement increases as the load decreases. And the largest improvement happens at the lowest load, in this case in Figure 2.5, 20% loading.

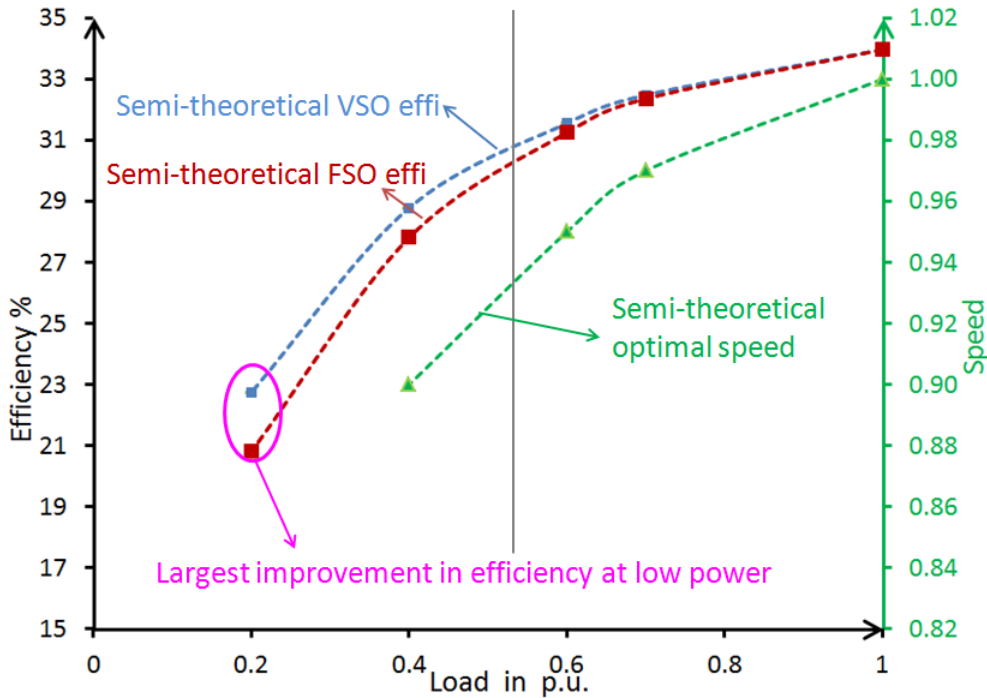


Figure 2.5 Semi-theoretical analysis of VSO on single-shaft GT efficiency

2.4.4 SEMI-THEORETICAL RESULTS OF TWIN-SHAFT GAS TURBINE

Similarly, following the same procedure of solving single-shaft gas turbine, the semi-theoretical results for a 0.96MW 20000RPM twin-shaft gas turbine are presented as in (2.22) and (2.23). Because of very limited access to the characteristic maps and data of a particular gas turbine, a twin-shaft gas turbine with different rating from single-shaft gas turbine was investigated.

$$\eta_{opt_2shaft} = -13.3L^2 + 31.1L + 17.4 \quad (2.22)$$

$$N_{opt_2shaft} = -19.9L^4 + 55L^3 - 55.1L^2 + 24.2L - 2.9 \quad (2.23)$$

These results (dashed lines) are plotted on Figure 2.6.

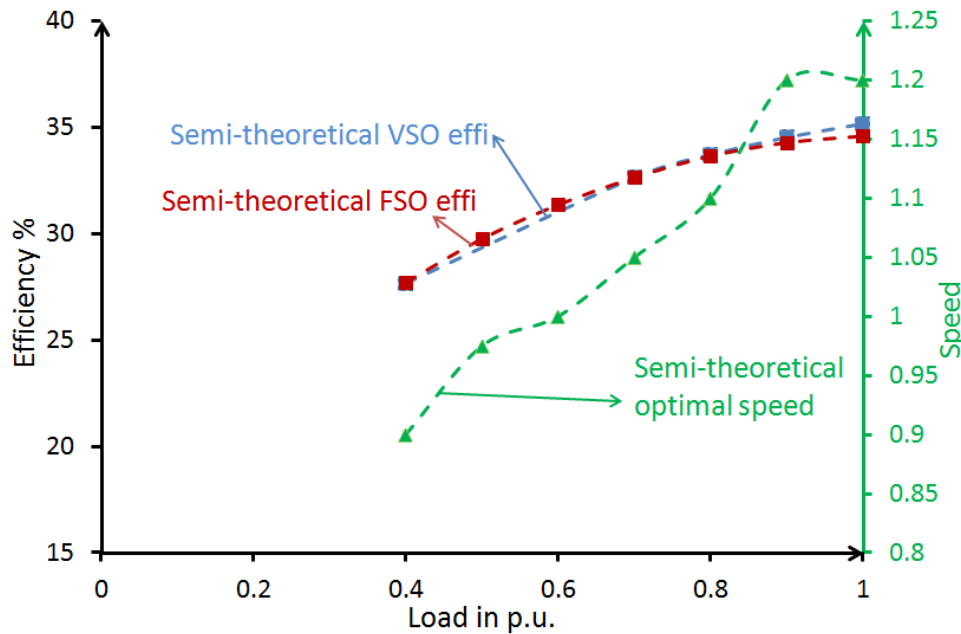


Figure 2.6 Semi-theoretical results of the impact of VSO on twin-shaft GT efficiency

2.5 MODELING AND SIMULATION

In this work, artificial turbine maps were used to model the gas turbine with the commercial software GasTurb [12], to evaluate its off-design performance.

The traditional linear modeling of gas turbine [7] [8] [9] are only valid for a small range around the design speed. In addition, modeling parameters are determined from tedious calculations and a tuning process using data obtained from field measurements. To study the wide range of operating speed other than the design speed, as well as part load condition, the gas turbine is modeled in GasTurb to verify the results obtained by the semi-theoretical analysis method described in the previous section. To determine the maximum efficiency points at different load conditions, from 0.2 to 1.0 p.u. both single-shaft and twin-shaft gas turbines were simulated for a range of shaft speed, 0.8 to 1.2 p.u. with increment of 0.01 p.u.

2.5.1 SINGLE-SHAFT GAS TURBINE MODELING

Figure 2.7 is the model set-up in GasTurb for a 5.71MW, 15808RPM single-shaft gas turbine power generation unit. The simulation results show, the impact of variable speed operation on single-shaft gas turbine efficiency as illustrated in Figure 2.8. To compare the results from semi-theoretical analysis, Figure 2.8 shows the results from both simulation and semi-theoretical analysis.

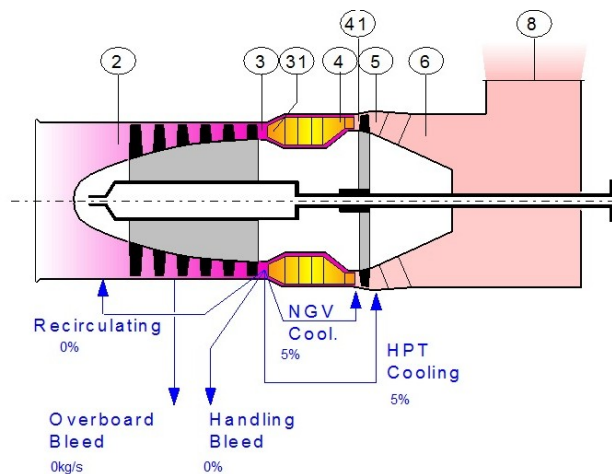


Figure 2.7 Single-shaft gas turbine as modeled in GasTurb

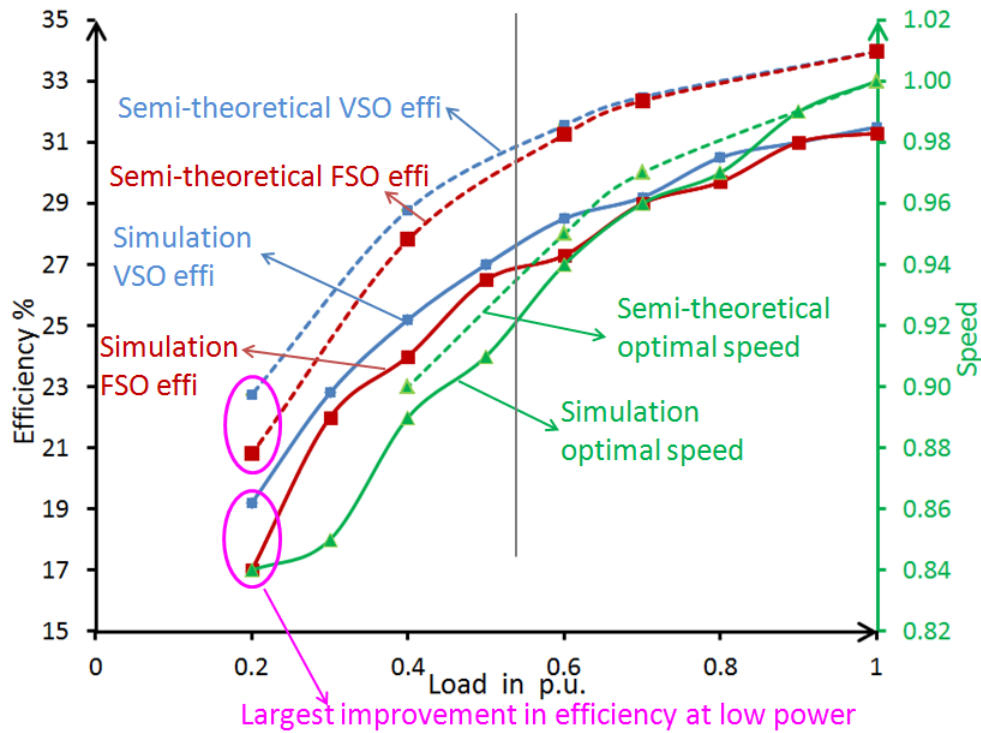


Figure 2.8 Impact of VSO on single-shaft GT efficiency (semi-theoretical and simulation)

In Figure 2.8, the green curve is the optimal speed corresponding to the optimal efficiency as indicated on the figure. The fixed speed efficiency curve is part-load efficiency at design speed, $N=1.0$ p.u. As can be seen on Figure 2.8, for lower power load demand, the gas turbine is more efficient at lower speed, as compared to fixed design speed. The semi-theoretical analysis results have similar trend as the simulation results, but the curves of semi-theoretical results being on the higher side in Figure 2.8.

The semi-theoretical analysis results were subjected to some modeling assumptions with respect to losses as discussed earlier while the simulation results for this case study considered several important parameters to replicate a gas turbine engine in working environment condition. The various parameters that were considered in this case study by

simulation were bleed, inlet/outlet losses, combustor part load calculation, shaft efficiency, component geometric properties, and other standard loss calculations. Otherwise, the overall graphical comparison shows an improvement of part-load efficiency for variable speed operation as compared to fixed-speed operation.

To better quantify the effect of variable speed operation, a variable, relative efficiency improvement is defined as

$$F_{index}\% = \frac{\eta_{VSO} - \eta_{FSO}}{\eta_{FSO}} \quad (2.24)$$

The relative efficiency improvement $F_{index}\%$ vs. output power of gas turbine is shown in Figure 2.9 and the blue line is the corresponding optimal speed.

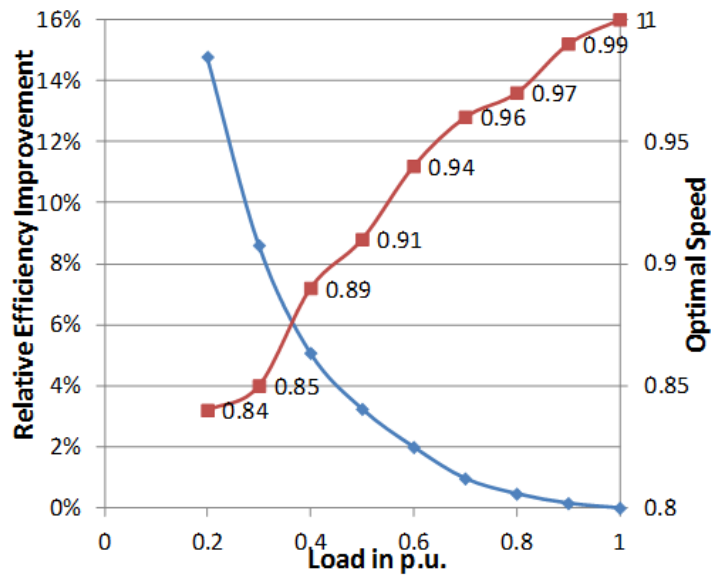


Figure 2.9 Relative efficiency improvement of single-shaft gas turbine at variable speed

For this specific single-shaft gas turbine, in simulation results as in Figure 2.8, the maximum absolute efficiency gain is 2.47% and its relative efficiency increased 14.77% at load with 0.2 p.u. where the optimal speed is 0.84 p.u. Because of physical limitations,

every gas turbine has its allowable specific operating speed range. For this modeled single-shaft gas turbine, the shaft cannot run at speed lower than 0.84 p.u. which shows up as non-convergences in simulation as indicated in the compressor map as Figure 2.10 and the turbine map as Figure 2.11. N means speed in p.u.; contours of constant efficiency are indicated with red dotted lines and corresponding numbers. The upper red dashed line is the surge line, which confines the feasible engine operating points. Also in Figure 2.10 and Figure 2.11, the green dot is the design point and the red dot is the operating point at speed of 0.83 p.u. The part-load efficiency improvement would be higher if the compressor had a wider range of operating speeds.

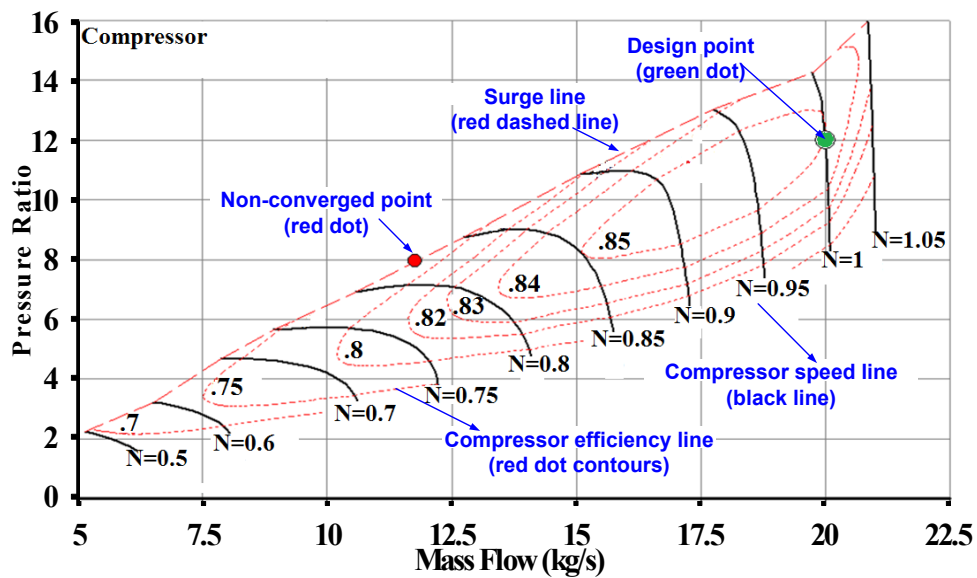


Figure 2.10 Compressor operating at speed N= 0.83 p.u. in single-shaft gas turbine speed

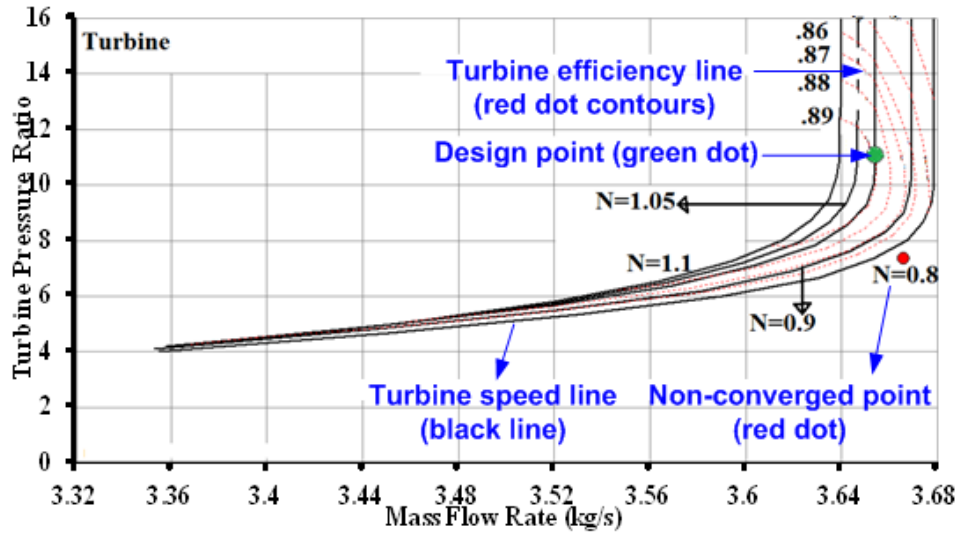


Figure 2.11 Turbine operating at speed $N=0.83$ p.u. in single-shaft gas turbine

Because almost two thirds of power generated by the turbine is used by the compressor, the turbine efficiency is relatively high as compared to the compressor efficiency. Therefore, adjusting the speed of the compressor corresponding to the load is the key to improve the part-load efficiency of the whole gas turbine. With different load conditions, the efficiency of the compressor running at fixed speed (design speed 1.0 p.u.) decreases along the speed line as can be seen in Figure 2.12. But in variable speed operation mode, the compressor efficiency decreases much less compared to fixed speed operating mode as shown in Figure 2.12, where the green dots are the optimal speed operating points and the green dashed line indicates variable speed operating trend for optimized efficiency when the load decreases.

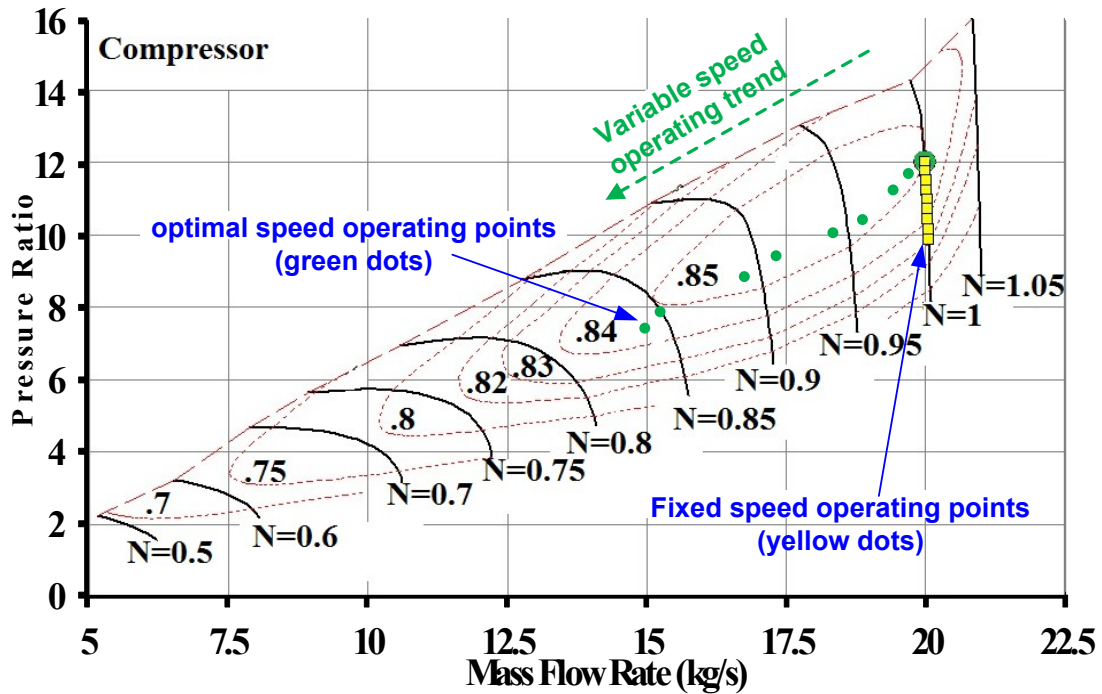


Figure 2.12 Compressor part load efficiency at fixed speed and variable speeds.

2.5.2 TWIN-SHAFT GAS TURBINE MODELING

Similarly to the modeling of single-shaft gas turbine, a 0.96MW 20000RPM twin-shaft gas turbine was modeled and variable speed operation of the free power turbine was simulated as well. The impact of variable speed operation on efficiency is illustrated in Figure 2.13. Compared to the modeled single-shaft gas turbine feasible operating speed range, from 0.84 to 1.2 p.u., the modeled twin-shaft gas turbine has a wider feasible operating speed range, from 0.8 to 1.2 p.u.

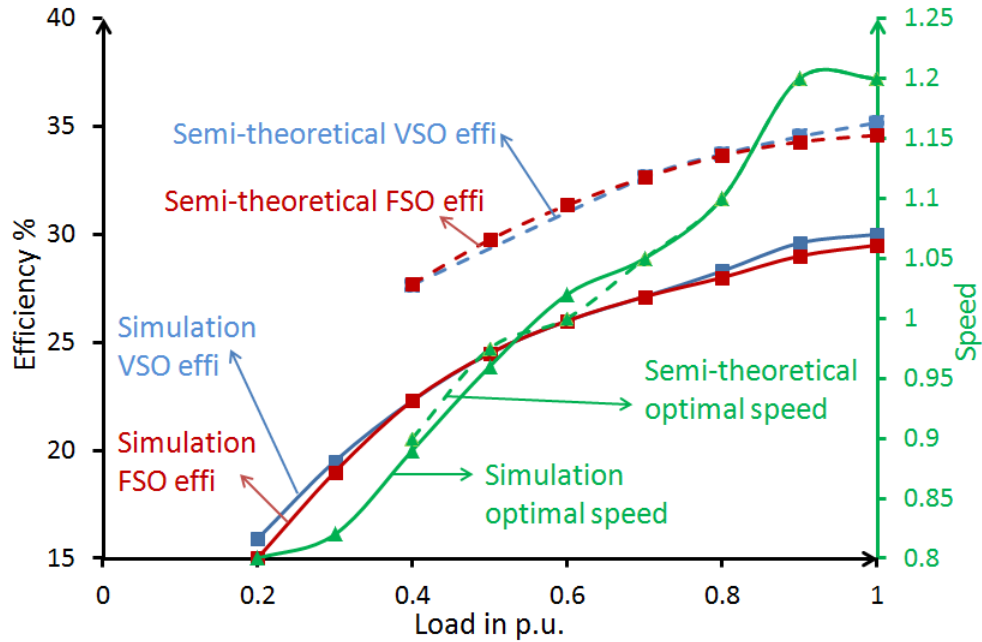


Figure 2.13 Impact of variable speed operation of twin-shaft gas turbine efficiency

Figure 2.13 shows that the maximum efficiency gain is 0.77% which increases from 15.03% to 15.8% at 20% of rated load with optimal speed $N=0.8$ p.u. For this load demand, running at variable speed operation may save up to 5.11% of fuel consumption. Running the free power turbine at variable speed operation only benefits the free power turbine itself, since the gas generator already runs at variable speed automatically based on the shaft load demand. The small change in efficiency with speed can also be explained by the free turbine power-speed curve shown in Figure 2.14 [14] which exhibits a speed range where power changes very little and which results in a small change in efficiency as well.

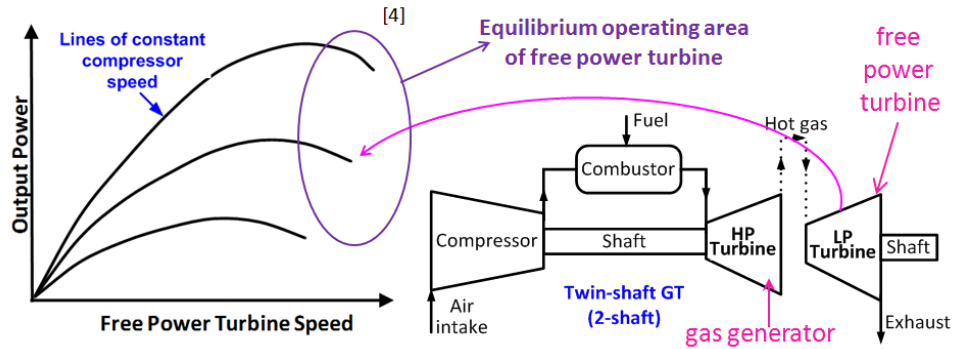


Figure 2.14 Free power turbine speed curves [14]

2.6 TEST ON GIVEN LOAD PROFILE

To further quantify the impact of variable speed operation of the single-shaft gas turbine, a load profile that illustrates the inherent part-load characteristics of propulsion in a navy ship is used to calculate total fuel consumption for constant and variable speed operations. Figure 2.15 (directly copied from [13]) shows a typical speed profile of a DDG51 ship (the speed profile is used as a surrogate for the electric power consumption profile on the basis that the propulsion system consumes the largest fraction of total electric power in an electrically-powered ship). The corresponding power profile is shown in Figure 2.16, in p.u., to illustrate the typical variation of propulsion power with ship speed. While the top speed of 30 knots requires full propulsion power, the time spent at that speed is less than 1%. This indicates that for the majority of the time, propulsion operates at part-load which will have a major impact on fuel consumption, and using variable-speed operation in this case has potential for significant fuel saving. The relationship between the efficiency η and the load power P_{shaft} (p.u.) at fixed speed as shown in Figure 2.7 can be expressed as a polynomial equation with curve fitting:

$$\eta = \sum_{i=0}^4 a_i P_{shaft}^i \tag{2.25}$$

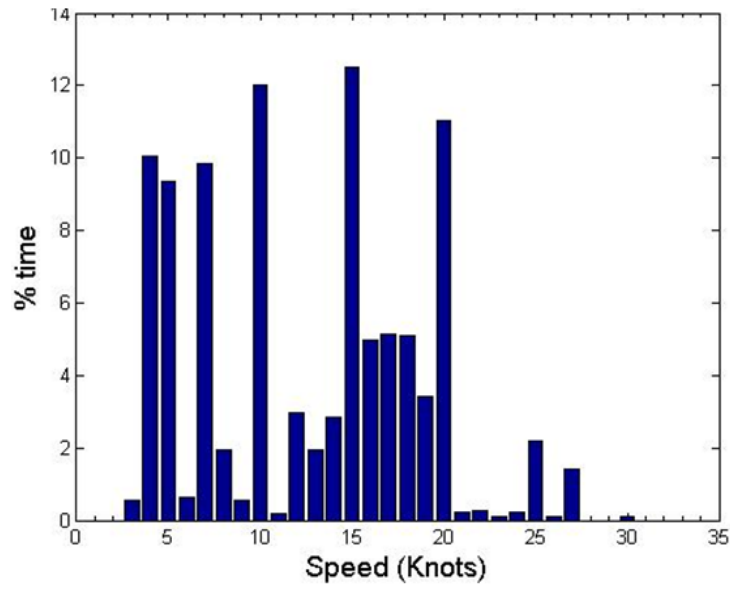


Figure 2.15 Typical propulsion speed profile of DDG-51 [13]

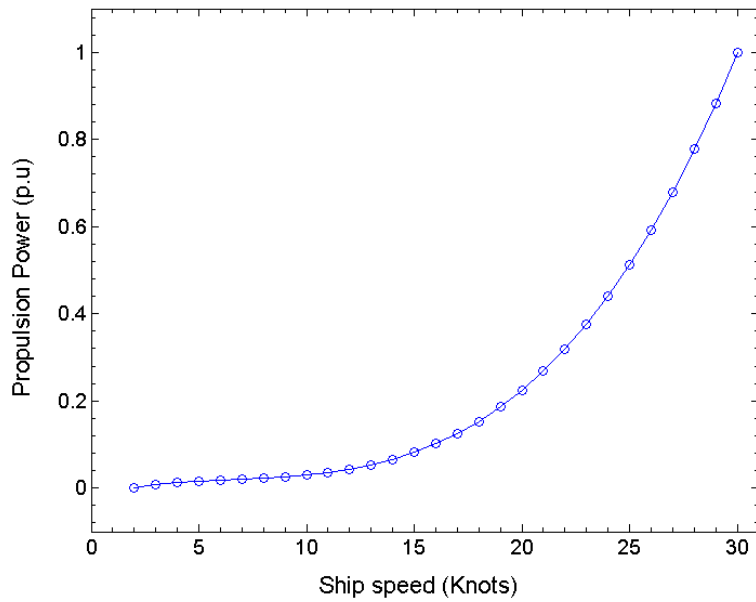


Figure 2.16 Variation of propulsion load power with ship speed

By scaling the load profile in Figure 2.16 to the rated power of the single-shaft gas turbine studied earlier, i.e. 5.71MW, and by constructing a 24-hour load profile that satisfies the speed and power profile shown in Figure 2.15 and Figure 2.16, total fuel consumption can be calculated for constant and variable speed operation of the gas turbine. For the load profile given in Figure 2.15, the total 1-day fuel consumption at variable speed and fixed speed operations are in Table 2.2. If a similar load profile was used, but with different power rating, the absolute fuel consumption reduction may be lower, but it is still 15.02% fuel consumption reduction per day as compared to the original fixed speed operation. The results are summarized in Table 2.2.

Table 2.2 Example of 1- day fuel consumption for constant and variable speed operation of gas turbine

Operation Mode	Fuel (kg)
Fixed Speed (N=1 p.u.)	1.32×10^4
Variable Speed	1.12×10^4
Fuel Consumption Reduced: 15.02% (1.98×10^3 kg)	

The calculation performed here, with a single-shaft gas turbine, was to illustrate the difference in fuel consumption between the two modes of gas turbine operation using a given load power profile that exhibits part-load characteristics as an example. It is important to note that in a typical ship there are several prime movers with different power ratings which can be adjusted so as to minimize fuel consumption when the load changes. In the multiple-engines system, if the number of on-duty turbines and their power sharing are optimized based on the load demand to improve overall system efficiency, then the

variable speed operation mode may not improve fuel saving as compared to the single engine case. However, if there is redundancy requirement in the system, then the variable speed operation would be very beneficial in terms of fuel saving like the investigated single-shaft turbine.

2.7 TORQUE CHARACTERISTIC COMPARISON

The impact of variable speed operation on the torque speed characteristics of single-shaft engines and on the gas generator of twin-shaft gas turbines are described in Figure 2.17 and Figure 2.18. The gas generator torque-speed characteristic for the twin-shaft gas turbine is similar to that of a single shaft gas turbine running at variable speed operation, which also explains in fixed speed operation, why the twin-shaft gas turbine gives relatively higher part-load efficiency compared to that of single-shaft gas turbines.

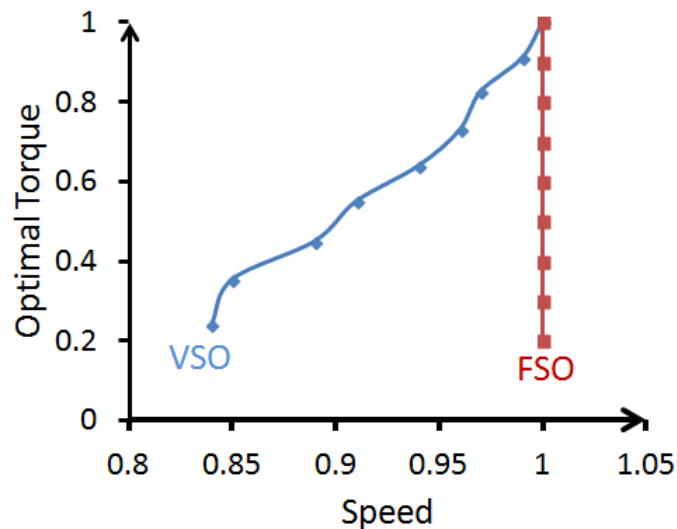


Figure 2.17 Torque characteristics of single-shaft GT

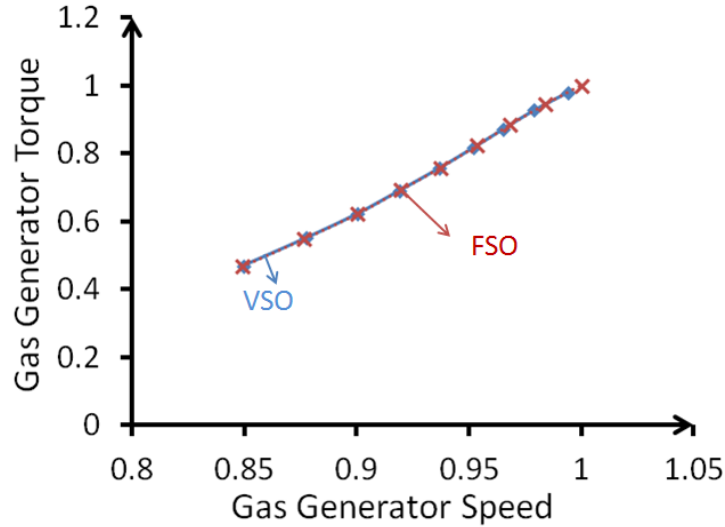


Figure 2.18 Torque characteristics of gas generator for a twin-shaft gas turbine

2.8 DISCUSSION AND CHAPTER SUMMARY

Variable speed operation has great benefit in improving part-load efficiency of a single-shaft gas turbine. It also provides better torque-speed characteristic for the reason that the compressor speed is adjusted to the power output. In contrast, the twin-shaft gas turbine doesn't benefit from variable speed operation as much as the single-shaft gas turbine because only the free power turbine itself benefits from the additional speed freedom – the gas generator already normally operates at variable speed. Considering that two thirds of the power produced by the gas turbine is consumed by the compressor and the turbine itself operates in a relatively high efficiency range, improving only the efficiency of the free turbine doesn't contribute significantly to improve the whole twin-shaft gas turbine efficiency. But in general, the variable speed operation does improve the part-load efficiency, especially for single-shaft gas turbines. Results of this analysis have been published in [56].

CHAPTER 3

COMPARISON OF POSSIBLE RECTIFIERS TOPOLOGIES IN MVDC POWER SYSTEMS

In the dc power generation chain, the dc system efficiency is decided by the gas turbine efficiency, the synchronous generator efficiency, as well as the rectifier efficiency. Chapter 2 presents the work about improving gas turbine efficiency by running it in variable speed operation mode. The synchronous generator efficiency improvement is described in Chapter 4, along with the integrated MVDC power system in variable speed operation mode. This chapter is a description of comparison of different rectifier topologies in MVDC power systems.

3.1 PROBLEM STATEMENT

DC power distribution offers several advantages over ac systems such as elimination of bulky transformers and the potential for variable speed operation which improves efficiency for part-load conditions, as described in the previous chapter. Medium voltage dc power distribution system is particularly suited for ship power systems because it provides high power density and the decoupling of generator speed and bus voltage [38].

Power generation modules in MVDC power systems typically consist of an ac power generation unit, such as a gas turbine coupled to a synchronous generator and an ac-dc rectifier. All these components have a significant effect on system efficiency and other performance metrics. The previous work presented in last chapter investigated the efficiency of gas turbine under different load conditions in both fixed speed operation and

variable speed operation [56]. This chapter addresses factors affecting the selection of the ac-dc rectifier for ship MVDC power systems including variable speed operation condition.

We consider only rectifiers that are appropriate for the voltage ranges typical for ship MVDC power systems. In MVDC ship power systems, dc bus voltages fall in the range of 1 to 35kV. IEEE Standard P1709/D11 (see Table 3.1) identifies preferred dc bus voltage levels [46]. For gas turbine driven generators, the recommended rated terminal voltages include 6.9kV, 11.5kV, 12.5kV, 13.8kV, and 14.4kV for 60Hz ac power systems [43]. We only consider boost type rectifiers to increase distribution voltage which leads to higher efficiency as compared to low voltage distribution systems. These factors suggest that a boost ac-dc rectifier, one having output dc voltage higher than the peak line-line ac voltage, is likely to be used in ship MVDC applications.

Table 3.1 Recommended MVDC voltage classes in ship system [46]

Variable	Maximum MVDC Class Rated Voltage (kV)
Already established classes	2 or ± 1
	5 or ± 2.5
Future design classes	10 or ± 5
	16 or ± 8
	22 or ± 11
	28 or ± 14
	34 or ± 17

3.2 COMPARISON FACTORS

First, the following factors that affect the complexity and cost of the rectifiers are considered:

- Complexity of rectifier control
- Number of switching devices
- Number/size of capacitors
- Number/size of inductors

We then examine several electrical performance factors, identified by Siebert, et. al. [42], as important when selecting ac-dc rectifiers for power systems. These factors fall into three categories: system level, dc side, and ac side.

The system level factor is:

- Rectifier efficiency (rated load and part load)

The dc side factors are associated with the quality of power provided to loads and include:

- dc voltage
- regulation constancy of dc bus voltage
- ripple of dc bus
- voltage regulation speed (overshoot and settling time in response to step load change)

The ac side factors include:

- ac input current distortion (Total Harmonic Distortion)

- power factor (or displacement power factor)
- ac voltage variation (magnitude, phase angle, and frequency)

Each of these factors except ac voltage variation (magnitude, phase angle and frequency) is considered. The factor of ac voltage variation is excluded because in a ship dc power system [38][41], the generators are not synchronized and the frequency and generator terminal voltage is not required to be fixed if a controlled rectifier is applied.

3.3 RECTIFIER OF TOPOLOGIES AND PARAMETERS

There are three types of boost ac-dc rectifiers available: diode rectifier with boost chopper (diode rectifier), three-level diode clamped voltage source converter (VSC), and modular multilevel converter (MMC). These three rectifiers are modeled and tested for a MVDC system with the parameters listed in Table 3.2. It is noted that here an available 4.16 kV synchronous generator is used. These parameters are typical of an electrical ship MVDC power system [38] [46]. Part-load efficiency is evaluated at 20% from rated frequency [56]; hence we analyzed the three models under ac side frequency of 0.8 p.u.

Table 3.2 Data of test system

Parameters	Value
rated line frequency (Hz)	60
line-to-line voltage (kV)	4.16
rated power (MW)	25
dc bus voltage(kV)	10
load change (p.u.)	1 to 0.25
range of operating line frequency (p.u.)	0.8 to 1

The THD of the converters is an important design factor because it causes losses and impacts the generator life [54] [55], and affects the sizing of filter elements in the converters. For this study, the three rectifiers considered are designed to have an ac side THD less than 5% under rated condition.

The maximum ripple and steady state voltage tolerance and deviation for the dc bus voltage are taken from IEEE standard 1662 [47] and listed in Table 3.3.

Table 3.3 Recommended requirements of voltage variations for dc system [47]

Parameters	Variations
Voltage tolerance (continuous)	$\pm 10\%$
Voltage cyclic variation deviation	5%
Voltage ripple (ac root-mean-square over steady dc voltage)	10%

3.3.1 DIODE RECTIFIER AND ASSOCIATED CONTROL

The diode rectifier with boost chopper first introduced in [48] is a two-stage ac-dc rectifier where a diode rectifier is connected with a dc-dc boost converter as in Figure 3.1. It consists of an input LC filter L_{a1} and C_f , a boost inductor L_{a2} , a three-phase diode rectifier, an active power factor stage, and a dc link capacitor. Among the three reviewed rectifiers, the diode rectifier with boost chopper has the simplest control structure as in Figure 3.2.

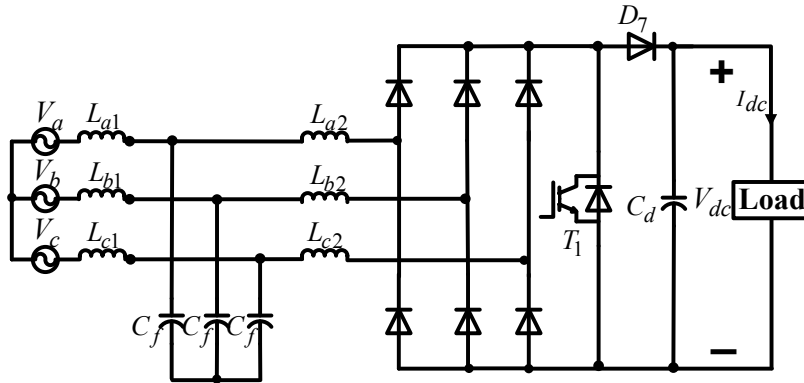


Figure 3.1 Diode rectifier with single-switch boost chopper

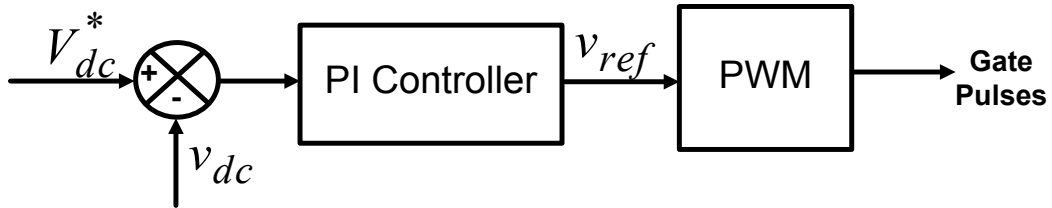


Figure 3.2 Diode rectifier with boost chopper control structure

3.3.2 VSC AND ASSOCIATED CONTROL

The three-level diode clamped voltage source converter [49] has six more diodes and one more capacitor to clamp the output terminal potentials to the neutral point. It produces fewer harmonics than that of a two level voltage source converter by using extra diodes and capacitor. The controllers applied in the rectifier with LCL filter are synchronous PI controller [50] as in Figure 3.3. The corresponding control diagram is shown in Figure 3.4.

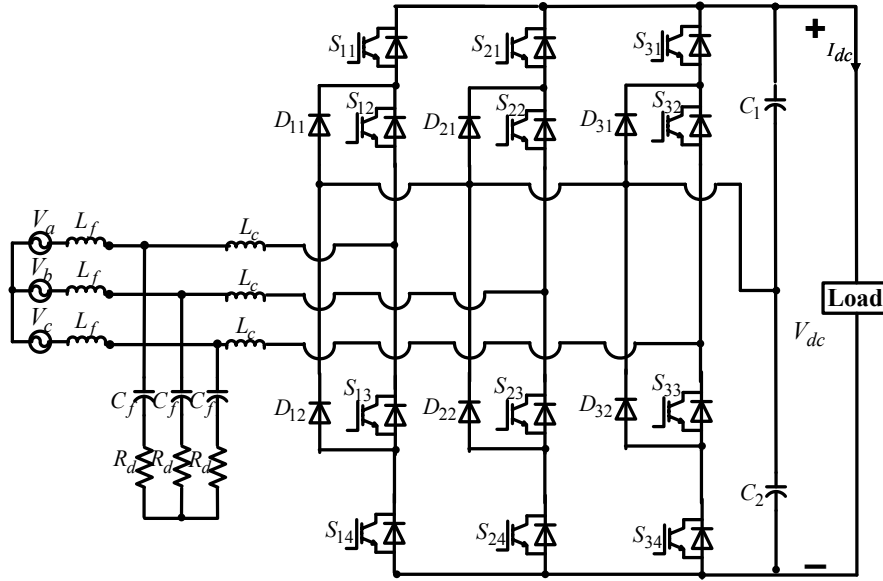


Figure 3.3 Three-level diode clamped VSC with LCL filter

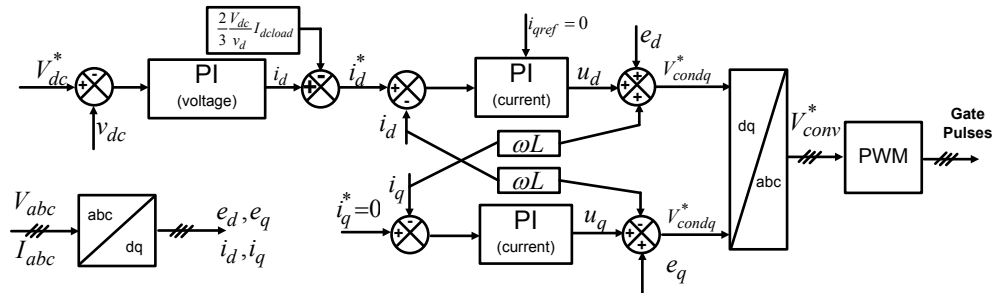


Figure 3.4 Control structure of three-level diode clamped VSC

3.3.3 MMC AND ASSOCIATED CONTROL

MMC, illustrated in Figure 3.5, was first introduced in 2001 [51]. It has three legs (corresponding to each phase) and each leg has two arms, upper arm and lower arm. Each arm has a total number of ‘n’ sub-modules and one inductor. Due to the modular structure, it can be extended to any level of power and voltage, and any number of voltage steps which then permits low THD of the input current. Sub-modules in one arm need not be

switched on or off at the same time so the stresses on the devices are significantly reduced which increases reliability of semiconductor devices [52]. For 25MW, 10kV MVDC system we modeled a 10-level MMC, which brings the sub-module voltage to 1kV- easily achievable with current semiconductor topologies Figure 3.6 is the control diagram including dc voltage controller and inner current controller. The applied modulation scheme is phase-shifted carrier-based PWM (PSC-PWM) with reduced switching-frequency voltage balancing algorithm [53].

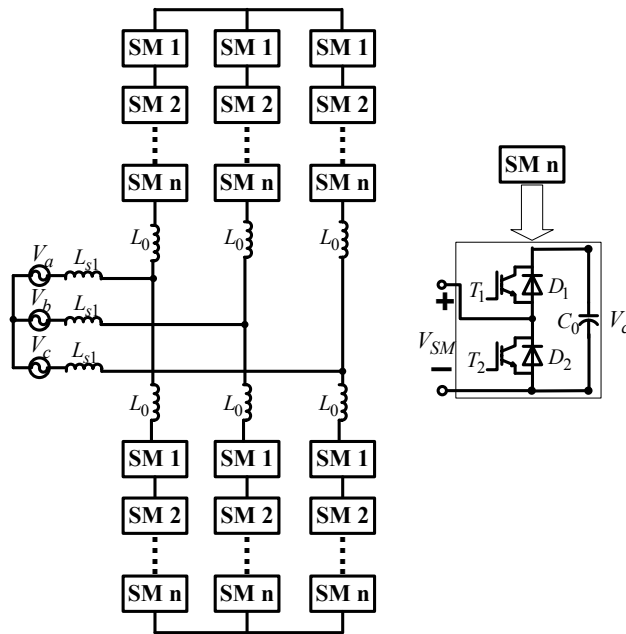


Figure 3.5 MMC

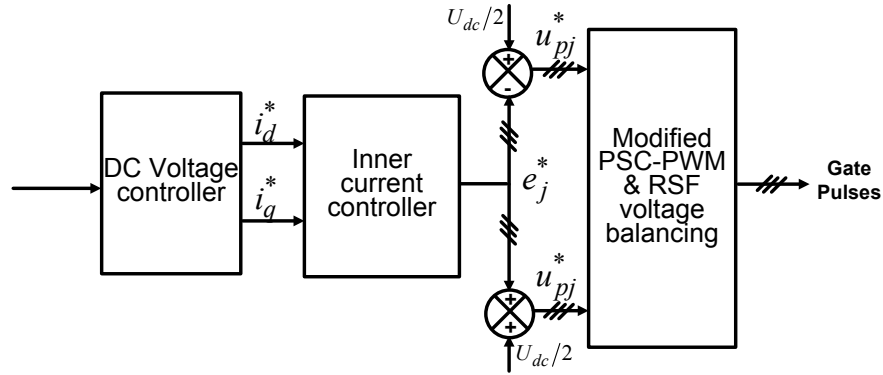


Figure 3.6 Control structure of MMC

3.4 RESULTSTS AND MERITS COMPARISON

3.4.1 COMPARISON OF NUMBER OF SEMI-CONDUCTOR DEVICES

Table 3.4 lists the numbers of semi-conductors for the three configurations of rectifiers. The diode rectifier (6-pulse) theoretically needs 1 IGBT and 7 diodes; the VSC theoretically needs 12 IGBTs and 6 diodes; and the MMC needs 120 IGBTs (for 10 level). However, because of the high power rating required, the diode rectifier needs 9 IGBTs and 140 diodes; the VSC needs 96 IGBTs and 48 diodes; and the MMC keeps the same number of IGBTs, 120. Even though, the base configuration of MMC requires more devices, it ends up with fewer devices for high power applications, which results in lower power losses as will be demonstrated next.

Table 3.4 Number of semi-conductor devices in rectifiers

	Diode Rectifier		VSC		MMC
	IGBTs	Diodes	IGBTs	Diodes	IGBTs
Type	ABB StakPak 5SNA	ABB HiPak 5SLD	ABB HiPak 5SNA	ABB HiPak 5SLA	ABB HiPak 5SNA

	2000K451300	1200J330100	3600E170300	3600E170300	3600E170300
# per stage	1	7	12	6	120
# of stages	group of 3 in series,	group of 4 in series,	group of 4 in series,	group of 4 in series,	1
	3 groups in parallel	5 groups in parallel	2 groups in parallel	groups 2 in parallel	
Total	9	140	96	48	120

3.4.2 COMPARISON OF INDUCTORS AND CAPACITORS

Table 3.5 describes the numbers and values of inductors and capacitors required for each rectifier. It is noted that a 10 level MMC needs total 60 sub-module capacitors and 6 arm inductors. Considering that dc side capacitors are electrolytic type, the corresponding weight is approximated as 0.2 kJ/kg [60][61]; and the ac side capacitors are polymer film type, with weight approximated as 0.4 kJ/kg [60][61]. As expected, MMC has the most total capacitors weight among the three rectifiers due to each submodule needing one capacitor. Assuming air core type with single layer [62], the total length for the corresponding inductor values are listed in Table 3.5. Diode rectifier has the longest wire (heaviest in mass), due to the high inductance value for ac side filter.

Table 3.5 Filters components comparison

System Parameter	Diode rectifier	VSC	MMC
L_f	778 μ H	83.2 μ H	N/A
R_f	5.9m Ω	0.63m Ω	N/A
C_f	400 μ F	147 μ F	N/A
R_d	N/A	0.1942 Ω	N/A
L_c	50 μ H	70 μ H	500 μ H
R_c	0.38m Ω	0.53m Ω	3.8m Ω
dc bus capacitor	3mF	4.2mF	10mF
C_0	N/A	N/A	26mF

L_0	N/A	N/A	0.5 μ H
R_0	N/A	N/A	0.38m Ω

3.4.3 RECTIFIER EFFICIENCY

The losses in the three reviewed rectifiers include losses in semi-conductor devices (IGBT and diode), and equivalent resistance losses of inductors. Losses in semi-conductor devices include conduction losses and switching losses. The conduction losses of IGBT and diode are calculated as (3.1) and (3.2). The resistance loss is calculated as (3.3):

$$P_{cond_T} = \frac{1}{T} \int_{t_0}^{t_0+T} v_{ce} i_c dt \quad (3.1)$$

$$P_{cond_D} = \frac{1}{T} \int_{t_0}^{t_0+T} v_f i_f dt \quad (3.2)$$

$$P_R = \frac{1}{T} \int_{t_0}^{t_0+T} R i_R^2 dt \quad (3.3)$$

P_{cond_T} : conduction loss of IGBT

P_{cond_D} : conduction loss of diode

P_R : resistance loss

v_{ce} : collector-emitter voltage of IGBT

i_c : collector current

v_f : diode forward voltage

i_f : diode forward current

v_R : voltage across the resistor

i_R : current across the resistor

t_0 : moment at that calculation starts

T: the cycle of calculation

According to datasheet [58] for a particular semi-conductor device, as shown in Figure 3.7, the collector-emitter voltage of IGBT, v_{ce} is a function of collector current, which is approximated as a polynomial function of i_C using curve fitting as in (3.4). Figure 3.9 displays that this polynomial equation represents the relationship of V_{CE} and I_C very well.

$$V_{CE} = a_0 + a_1 I_{ce} + a_2 I_{ce}^2 + a_3 I_{ce}^3 + a_4 I_{ce}^4 \quad (3.4)$$

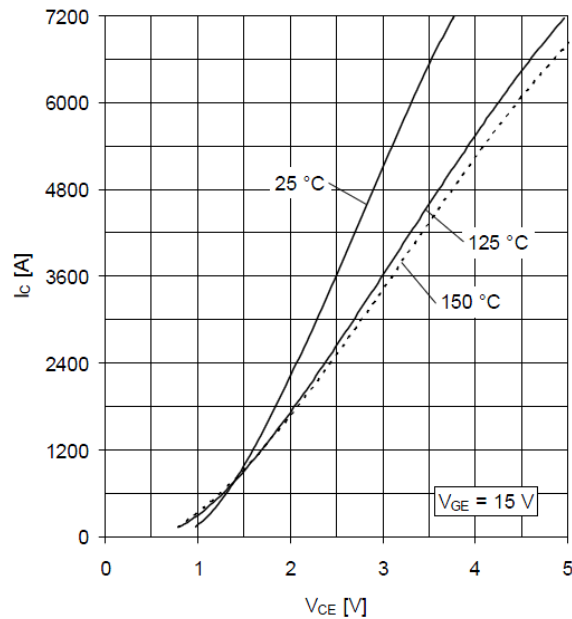


Figure 3.7 Typical V_{ce} and I_c characteristic of IGBT [58]

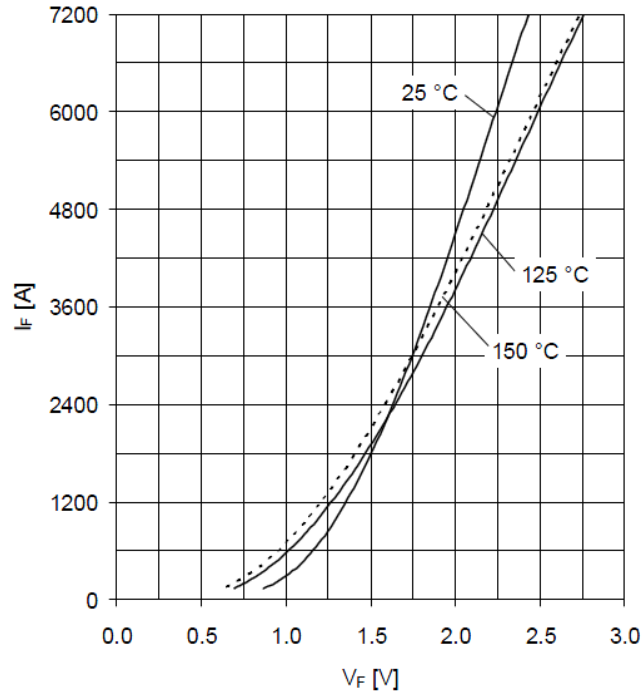


Figure 3.8 Typical V_f and I_f characteristic of diode [58]

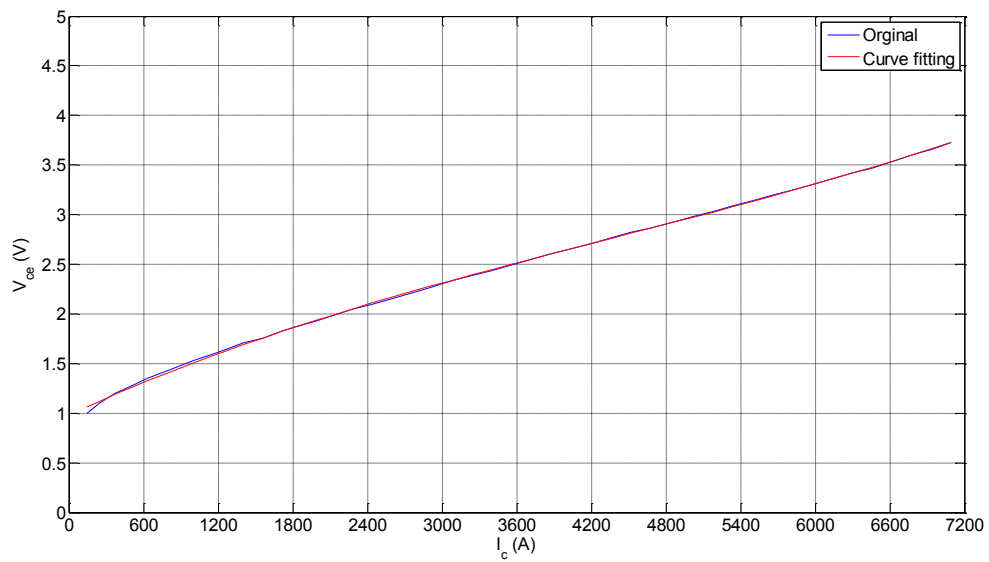


Figure 3.9 Curve fitting of V_{ce} as a function of I_c

To The relationship between V_f and i_f , is obtained from the datasheet as in Figure 3.8. V_f is approximated as a function of I_f using curve fitting as (3.5), which matches the original curve very well as in Figure 3.10.

$$V_f = a_0 \cdot (a_2 + \sqrt{I_f}) + a_3 + a_4 \cdot I_f \quad (3.5)$$

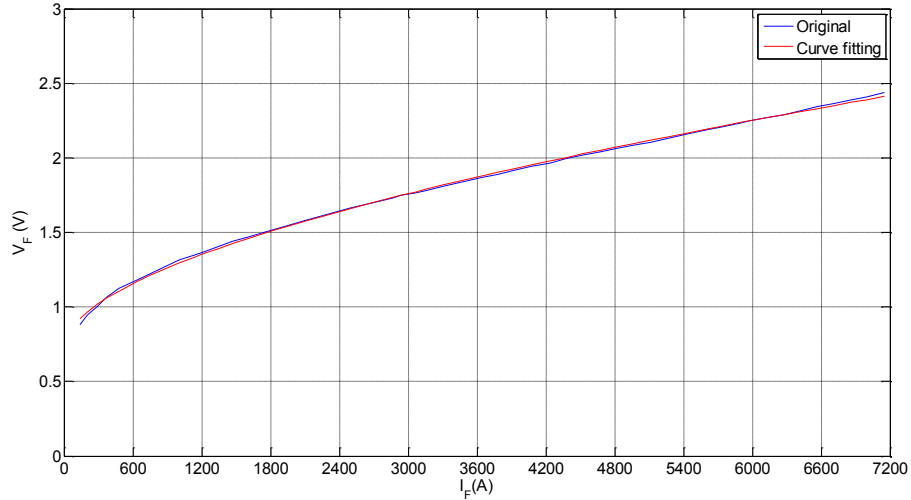


Figure 3.10 Curve fitting of V_f as a function of I_f

The switching losses of IGBT include the turn on and turn off loss of IGBT. The switching loss of diode is mainly reverse recovery loss; turn-on losses of diodes are negligible. These losses (per cycle) are approximated as polynomial functions of current as in (3.6) (3.7) and (3.8)

$$W_{on} = a_0 + a_1 I_{ce} + a_2 I_{ce}^2 + a_3 I_{ce}^3 + a_4 I_{ce}^4 \quad (3.6)$$

$$W_{off} = a_0 + a_1 I_{ce} + a_2 I_{ce}^2 \quad (3.7)$$

$$W_{rec} = a_0 + a_2 (I_f - b)^2 + a_3 I_f^3 \quad (3.8)$$

Based on the energy loss above, the equivalent average loss is calculated as

$$P = \frac{W}{T} \quad (3.9)$$

where P power and W is energy.

Efficiency of a rectifier is defined as

$$\eta = \frac{P_{dc}}{P_{dc} + P_{lossT}} \quad (3.10)$$

where P_{dc} is dc bus load power and P_{lossT} is total loss of a rectifier caused by semiconductor devices and filters.

Following above procedure, the efficiencies of the three reviewed rectifiers under different load conditions are shown in Figure 3.11.

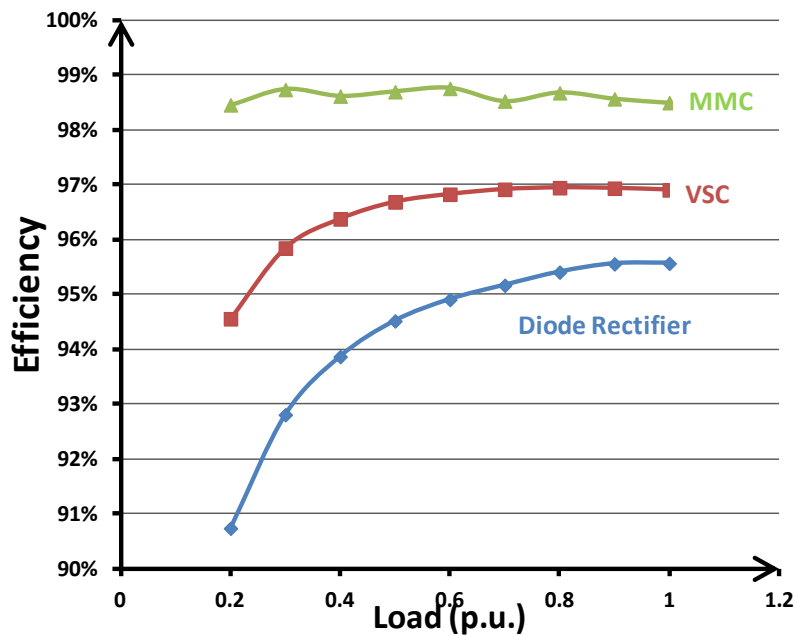


Figure 3.11 Efficiency of rectifiers at fixed speed

It should be noted that MMC has highest efficiency compared to diode rectifier and VSC even though it has the most semiconductor devices from rectifier configuration

topology in Figure 3.5. The higher efficiency is due to the low switching frequency and no need of series connection of semi-conductors. It is also noted from Figure 3.11, the efficiency of MMC is relatively not as dependent on the load compared to that of VSC and diode rectifiers.

3.4.4 DC VOLTAGE FACTORS

This section discusses the dc bus factors of the three rectifiers. The performance is shown via simulation in which there is a step load change from full load to 25% load at $t = 2.5s$. The considered dc bus factors including peak-peak voltage ripple defined as (3.11) and dc bus voltage overshoot during transient defined as (3.12), and the time required to return to steady state during transient events.

$$V_{rpp}\% = \frac{V_{rpp}}{V_{dc}} \quad (3.11)$$

$$overshoot\% = \frac{V_{dcpeak} - V_{dc}}{V_{dc}} \quad (3.12)$$

where V_{dc} is the mean value of dc bus voltage.

Figure 3.12 shows the dc bus voltage of the three rectifiers. It shows that MMC has the best dc bus performance, especially during transients when there is a load change. Load conditions have much less influence on the dc bus for MMC compared to the other two rectifiers. Table 3.6 lists the voltage ripple on the dc bus and the overshoot and settling time in response to a step change in the load. For nearly all cases the MMC had the least ripple and fastest response to load change.

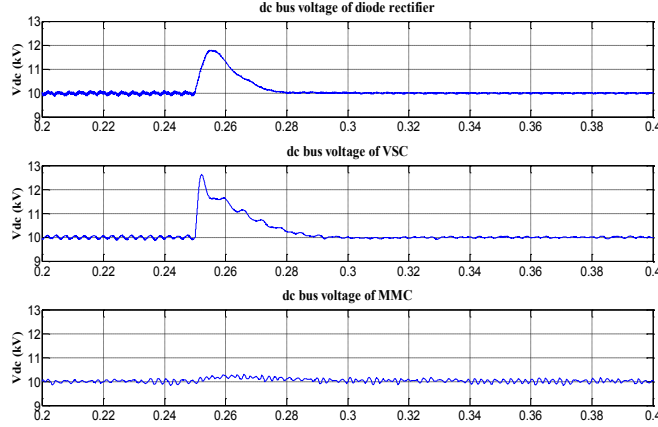


Figure 3.12 Waveforms of dc bus voltage

Table 3.6 DC bus voltage performance

	dc bus voltage peak-peak ripple			overshoot (75% load change)	time required to be in steady state (ms)
	full load	25% load			
		f=1 p.u.	f=0.8 p.u.		
diode rectifier	2%	5%	4%	18.3%	20
VSC	2%	1%	5%	26.5%	24
MMC	1.8%	1.8%	2%	3.2%	negligible

3.4.5 AC INPUT VOLTAGE AND CURRENT DISTORTION (TOTAL HARMONIC DISTORTION)

The THD of both voltage and current under both rated and partial load conditions are listed in Table 3.7. THDs of voltage and current on the generator stator side have great impact on generator insulation life, and increase heating and decreased efficiency respectively [54] [55]. With THD ranging less than 15%, the generator insulation life and efficiency decrease linearly as THD increases [54] [55]. As stated earlier, the three rectifiers are designed to meet THD less than 5% under rated condition. However, the

MMC provides the cleanest voltage and current (lowest THD) of the three rectifiers. It is also notable that the MMC has the same THDs of voltage and current for different load conditions, which suggests it is well suited for systems that run at part-load.

Table 3.7 THD of phase voltage and current

	THD-Voltage			full load	25% load	
	full load	25% load			f=1 p.u.	f=0.8 p.u.
		f=1 p.u.	f=0.8 p.u.			
diode rectifier	1.1%	0.3%	0.3%	1.1%	0.3%	4.2%
VSC	3.8%	4.1%	4%	3.8%	4.1%	10%
MMC	0.8%	0.8%	0.9%	0.8%	0.8%	4.6%

3.4.6 DISPLACEMENT POWER FACTOR (DPF)

Figure 3.13 shows the simulated displacement power factor of the rectifiers. Both VSC and MMC have the desired unity displacement power factor, while the displacement power factor for the diode rectifier decreases greatly when the load decreases.

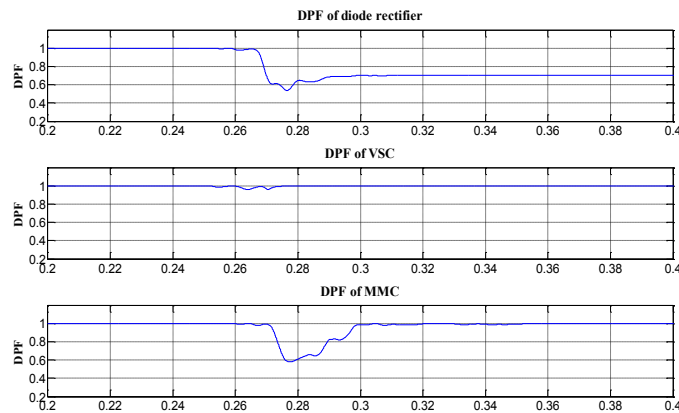


Figure 3.13 DPF of rectifiers

3.5 VARIABLE SPEED OPERATION

DC distribution system permits variable speed operation of the prime movers which offers advantages in part-load efficiency [56]. This section discusses the three rectifiers' performance in variable frequency operation. In this study, the frequency of three-phase ac voltage source is set to 0.8 p.u. when operating at 25% loading, because the optimal speed for low load condition is as low as 0.8 p.u.

3.5.1 DIODE RECTIFIER

Variable frequency operation can greatly improve the part-load DPF of diode rectifier. In this situation, it increases to 0.7 from 0.6, which reduces the peak phase current by 18% from 2111A to 1735A as shown in Figure 3.14. Under 25% loading, the blue waveform is current under fixed frequency operation, while the red one is current under variable frequency, i.e. 0.8 p.u.

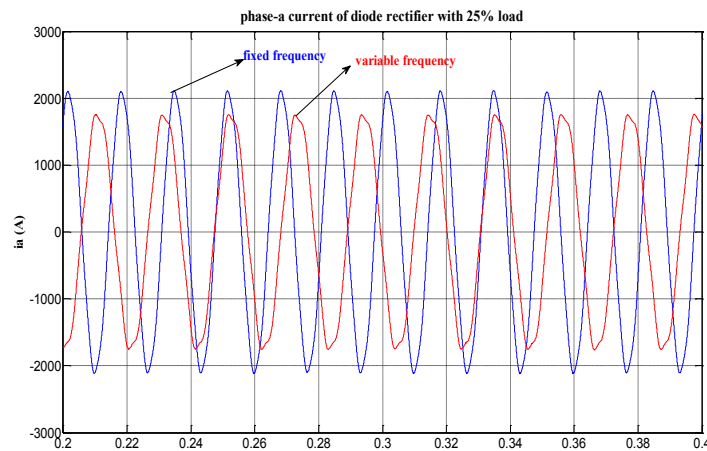


Figure 3.14 Phase current of diode rectifier in fixed frequency operation and variable speed operation

3.5.2 VSC AND MMC

Variable frequency operation with VSC and MMC has little influence on DPF, which suggests that both three-level VSC and MMC are suitable for variable speed operation in a dc distribution power system.

3.5.3 EFFICIENCY

Variable speed operation does not affect rectifier efficiency (see Figure 3.15) compared to fixed speed operation.

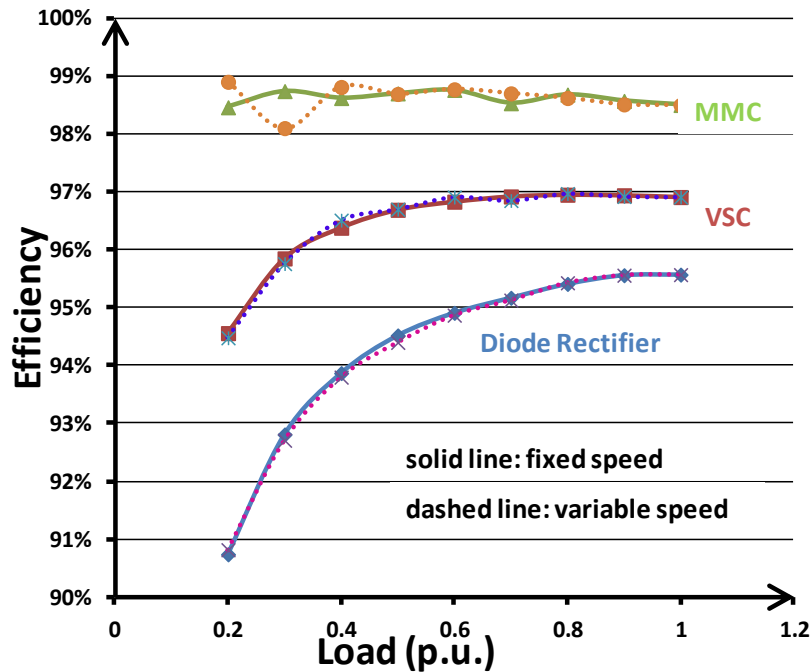


Figure 3.15 Efficiency of diode rectifier, VSC, and MMC in fixed frequency operation and variable speed operation

3.6 MERITS COMPARISON SUMMARY

From the analysis above, it is shown that each rectifier has its own advantages and disadvantages, which are summarized in Table 3.8. Figure 3.16 and Figure 3.17 show a direct comparison of passive components inductor and capacitor. In Figure 3.16, the MMC

inductor is scaled to 100 times for comparison, which shows that the inductor of MMC is also negligible compared to diode rectifier and VSC. But MMC's capacitor weight is about 6 times that of VSC and about 8 times that of diode rectifier. Compared to 4 kHz switching frequency of diode rectifier and VSC, MMC's switching frequency for each device is 250 Hz, resulting in 25 HZ equivalent switching frequency for each arm for 10 level MMC. It is noted that increasing the carrier frequency of MMC will further decrease the values of passive components.

Table 3.8 Merits comparison summary

	diode rectifier	VSC	MMC
Control Complexity	Low	Intermediate	High
ac side LCL filter	778 μ H 400 μ F 50 μ H	83.2 μ H 147 μ F 70 μ H	N/A
arm inductor	N/A	N/A	0.5 μ H 6 inductors Total 3 μ H
Sub-module capacitor	N/A	N/A	26mF 120 capacitors Total 3.12 μ F
dc bus capacitor	3mF	4.2mF	10mF
Number of switches	149	144	120
Total capacitor mass (kg)	846	1077	6400
Total inductor wire length (m)	198	85.8	154.3
Efficiency at rated condition	95.58%	96.91%	98.5%
Part load efficiency at fixed speed	Low	Intermediate	High

Dc bus voltage peak-peak ripple	1.8%	2%	1.8%
Dc bus voltage overshoot	18.3%	26.5%	3.2%
Voltage regulation speed	Intermediate	Intermediate	Fast
THD I/V	Better	good	Best
DPF	Unity only at rated load	Unity at any load	unity at any load
Switching frequency	4KHz	4KHz	250Hz

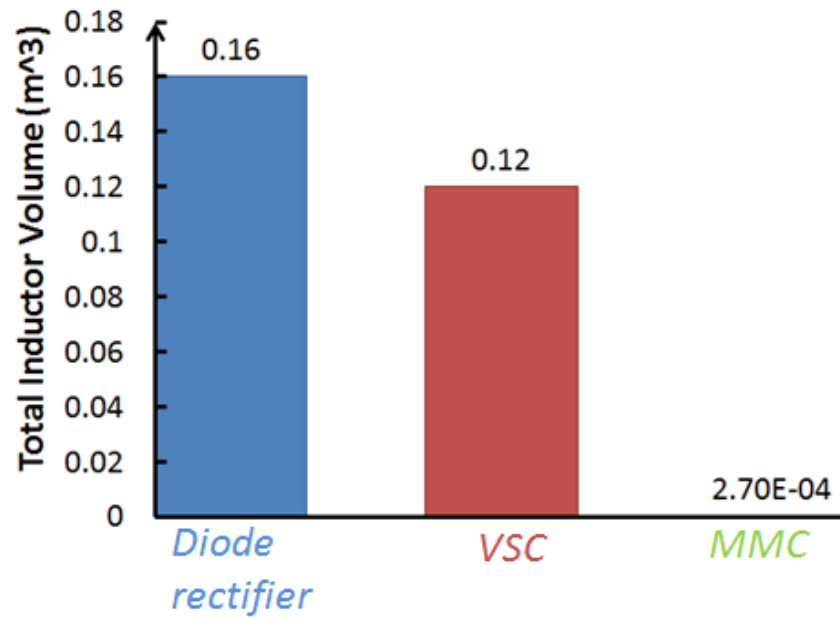


Figure 3.16 Total inductor volume comparison

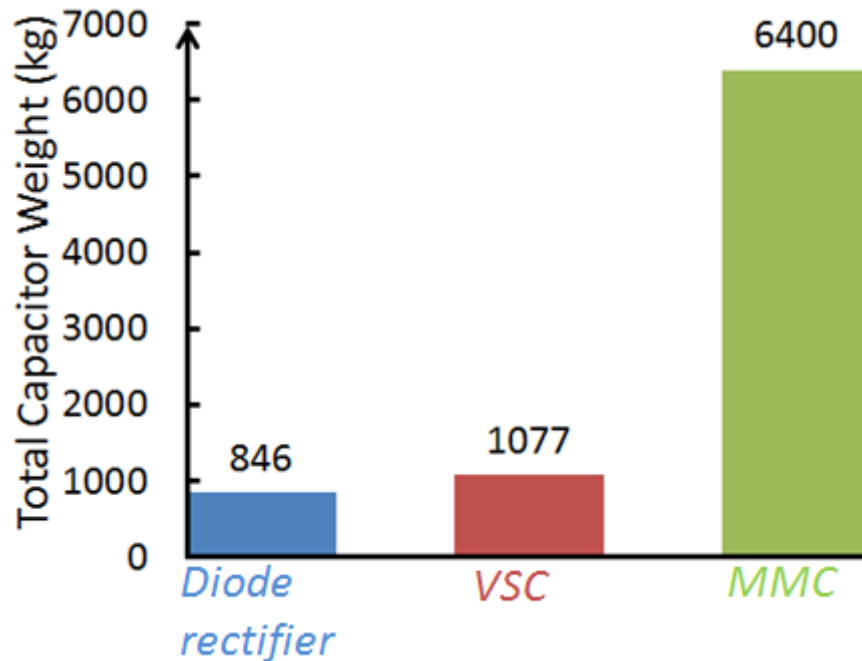


Figure 3.17 Total capacitor weight comparison

3.7 DISCUSSION AND CHAPTER SUMMARY

Our extensive investigation of three types of boost ac-dc rectifiers for MVDC power systems, including diode rectifier with boost chopper (diode rectifier), three-level diode clamped voltage source converter (VSC), and modular multilevel converter (MMC) gives a series of merits comparison to clarify the advantages and disadvantages of the three boost type converter. As expected, MMC provides the best dc bus voltage performance including voltage ripple, overshoot, and settling time. However, the control strategy of MMC is the most complicated, while diode rectifier has the simplest control strategy. Both VSC and diode rectifier have big voltage overshoot during load change. On the ac side performance, MMC is also the best among the three reviewed rectifiers in terms of voltage and current distortions. Diode rectifier also has better ac voltage and current performance

than that of VSC, but at the price of large LCL filters. The ac side L filter is almost 10 times of that of VSC. For DPF, all three rectifiers are able to provide unity DPF under rated load condition. Due to their inherent advantages of operating as active rectifiers by using IGBTs, MMC and VSC can provide unity power factor for all load conditions, but the DPF of diode rectifier decreases as load decreases, and is as low as 0.61.

For efficiency, MMC is the most efficient in MVDC system although it has the most components due to its modular topology. This is because both diode rectifier and VSC need series connection to meet the MW power requirements. And the MMC has the lowest switching frequency 250Hz compared to 4 kHz of diode rectifier and VSC. MMC's sub-modules in one arm do not need to be switched on or off at the same time, that brings lower average switching frequency [51] [52]. The lower switching frequency of the semiconductors leads to low converter losses. Moreover, the efficiency of MMC is almost independent on the load conditions, while the other two rectifiers' efficiency decreases as the load decreases. For variable speed operation, neither MMC nor VSC has influence on ac and dc side performances. But variable speed operation can greatly increase DPF of diode rectifier, which reduces the ratings of components, cables, measurement instrument, etc. For passive component consideration, MMC has negligible inductor space requirement compared to the other two, but requires about 6 to 8 times the capacitor weight needed for the two other rectifiers.

CHAPTER 4

INTEGRATED MVDC POWER SYSTEM IN VARIABLE SPEED OPERATION MODE

4.1 PROBLEM DESCRIPTION AND BACKGROUND

Investigation of variable speed operation has been done in both gas turbine engine and possible ac-dc rectifier topologies in the previous two chapters. The feasibility of variable speed operation in efficient MVDC power generation depends on the integration of dc power generation units including gas turbine, generator, and rectifier. This chapter develops a procedure to control MVDC power system in variable speed operating. It analyzed the steady state efficiency improvement and the dynamic performance during transients.

As mentioned earlier, distribution of power in dc forms offers several advantages over ac such as elimination of bulky transformers and the potential of variable speed operation of power generation source [36][37][38]. Additionally, the decoupling of dc bus voltage and ac frequency in dc power systems enables operation of each generating asset at the speed most optimal for its particular loading. Power generation in MVDC power systems typically consists of an ac power generation unit, such as a gas turbine coupled to a synchronous generator, and an ac-dc rectifier as in Figure 4.1. All of these components have a significant effect on system efficiency and on other performance metrics. As presented in Chapter 2 and Chapter 3, previous work included investigation of part-load

efficiency improvement of gas turbines [56] and comparison of possible rectifier topologies in MVDC power system [63].

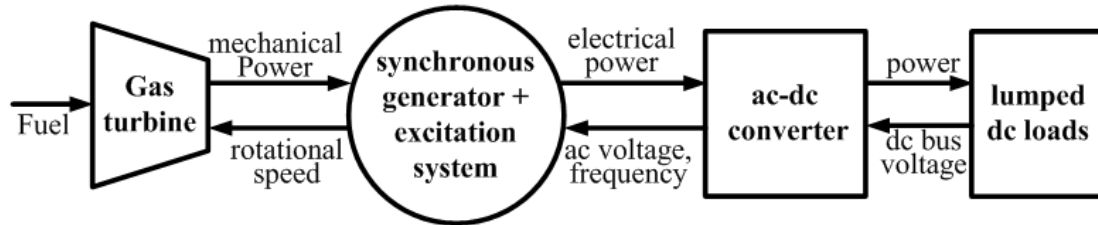


Figure 4.1 Diagram of a MVDC power system

In Chapter 2, we investigated the efficiency of gas turbine under different load conditions in both fixed speed operation and variable speed operation including both single-shaft and twin-shaft variants by semi-theoretical analysis, and simulation validation. The results show significant opportunities to improve part-load efficiency in electrical power generation applications that permit variable speed operation. Efficiency improvement increases as load decreases and the improvement is larger for single-shaft engines than for twin-shaft engines. For example, when operating at 20% loading, adjusting the engine speed can improve fuel efficiency by 14% for single-shaft gas turbines, and by 2% for twin-shaft gas turbines. With a load profile representative of a typical propulsion profile for a DDG 51 ship, 15% reduction in fuel consumption can be achieved by running a gas turbine in variable speed operation, as compared to fixed speed operation.

In [63] we compared diode rectifier, VSC, and MMC in terms of complexity of control strategy, number of switching devices, number/size of inductors and capacitors, the dc bus voltage performance (peak-peak voltage ripple, overshoot, and settling time after a load

change), the total harmonic distortion (THD) of the ac side input current and voltage, displacement power factor (DPF), efficiency for different load conditions, and performance under variable ac frequency operation. MMC is found to be the most efficient and it remains efficient almost independent of load conditions. The comparison shows that MMC provides the best dc bus performance, including low overshoot, and low ripple. All the advantages of MMC are paid by the price of adding more capacitors into the system in terms of both number of capacitors and total weight. All the three compared rectifiers can provide unity DPF under rated condition, but the DPF of diode rectifier decreases as load decreases while VSC and MMC can provide unity DPF independently of load condition. Balancing performance and cost, VSC is a preferable choice as a rectifier topology for use in MVDC power systems.

The losses of synchronous generator include friction loss, windage loss, iron loss, and copper losses of both rotor and stator as in Figure 4.2. As in Figure 4.2, some losses are dependent on frequency and some are not. For fixed speed operation, the efficiency of synchronous generator is a function of the electric power load only [64][5][44], like a polynomial function as in Figure 4.3. In variable speed operation, the synchronous generator efficiency is a function of both electrical load and its running speed [64][5]. Variable speed operation of generator has been applied in wind turbine generators [65] and diesel engine driven power generation [66] in distribution power generation area to improve system efficiency. It can be estimated that the efficiency curves of synchronous generator is a series of similar curves like in fixed speed operation, which is available from calculations of manufacture data as in Figure 4.4.

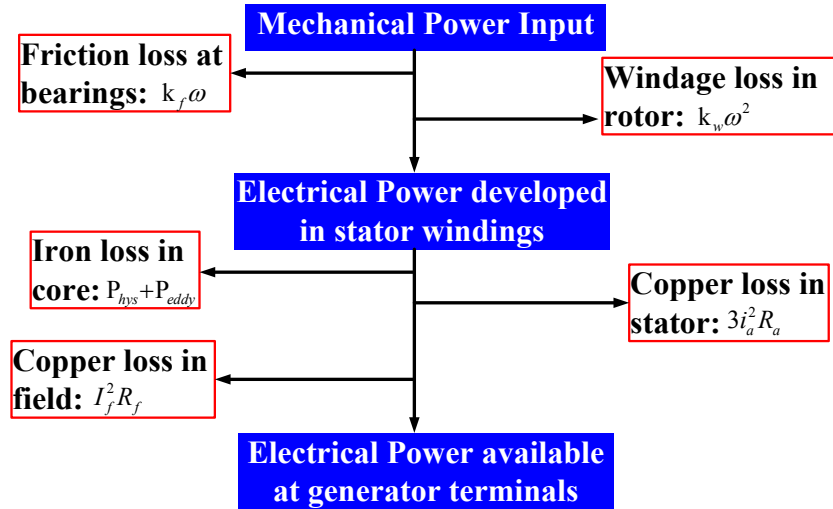


Figure 4.2 Power flow chart of synchronous generator

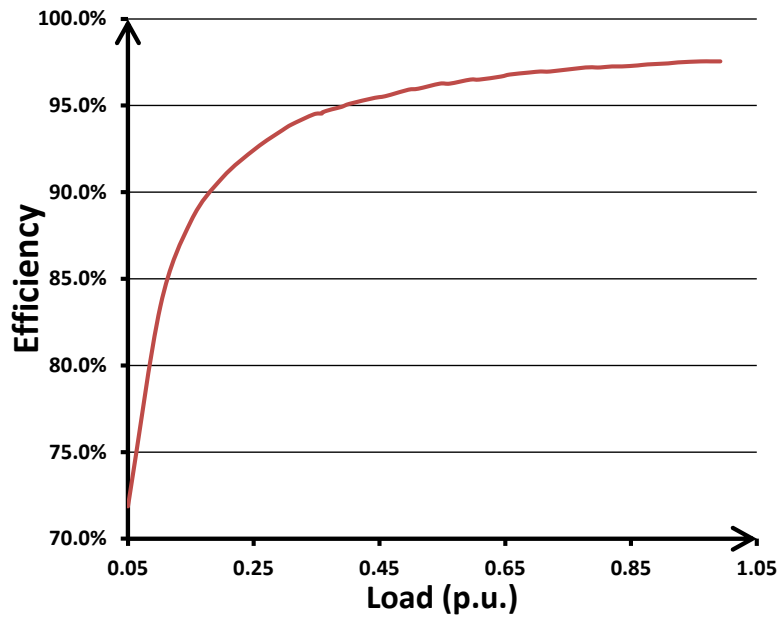


Figure 4.3 Typical efficiency curve of a synchronous generator at fixed speed

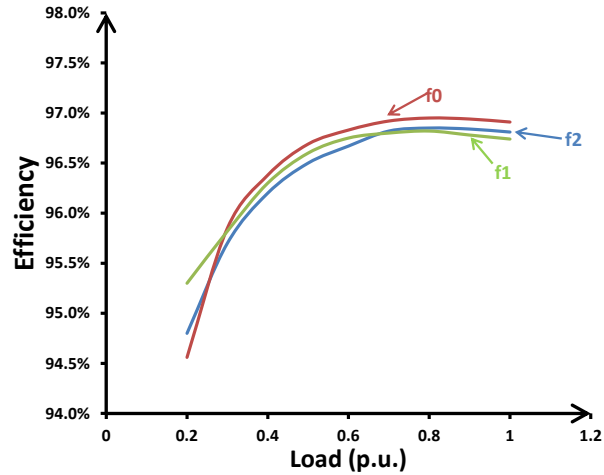


Figure 4.4 Efficiency of synchronous generator vs. electric load at different speeds

In this chapter, we modeled the integrated MVDC system comprising the three units above, analyzed the steady-state efficiency, and developed a procedure for appropriate control of the variable speed MVDC power system.

4.2 APPROACHES AND ANALYSIS RESULTS

In a gas turbine driven MVDC system, the main loss of dc power generation is due to the low efficiency of gas turbine when operating at part-load. Specifically, the gas turbine efficiency decreases significantly as load decreases, and running the MVDC system at the speed where the gas turbine efficiency is optimal, and corresponding to a specific load is the key to generate dc power in the most efficient way. Previous work in Chapter 2[56] developed a procedure to find the optimal speed of gas turbine corresponding to different shaft power levels. Ultimately, the goal is to develop a procedure to obtain the optimal speed corresponding to the dc bus load power. Then, the obtained optimal speed would be a reference speed for the gas turbine governor control as depicted in Figure 4.5.

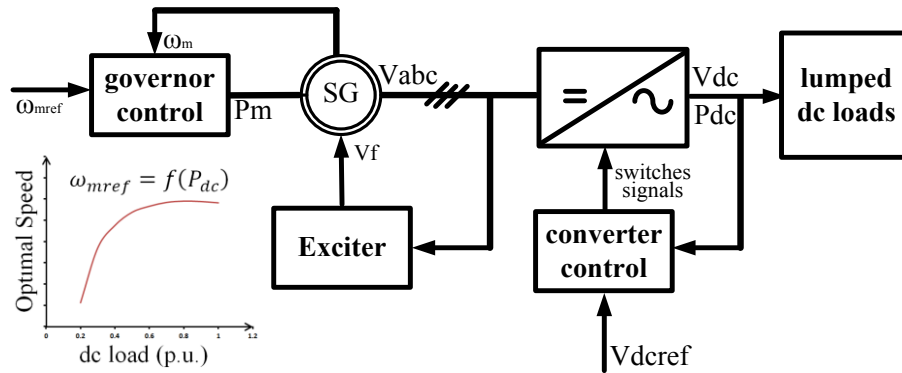


Figure 4.5 Control diagram of MVDC power system

Table 4.1 Data of test system

Parameters	Value
rated line frequency (Hz)	60
line-to-line voltage (kV)	4.16
rated power (MW)	25
dc bus voltage(kV)	10
load change (p.u.)	1 to 0.25
range of operating line frequency (p.u.)	0.8 to 1

4.2.1 VARIABLE SPEED EFFICIENCY OF GAS TURBINES

As demonstrated in Chapter 2, decreasing the speed as load decreases can improve the compressor efficiency greatly as in Figure 2.12. The optimal efficiency and speed curve for a single-shaft gas turbine in [56] is in Figure 2.8. The optimal efficiency and corresponding optimal speed can be approximated as a polynomial function of shaft power load as in (4.1) and (4.2).

$$\eta_{opt_gt} = 28.06P_{gt}^3 - 71.01P_{gt}^2 + 64.44P_{gt} + 12.48 \quad (4.1)$$

$$N_{opt_gt} = 1.4931P_{gt}^4 - 4.170P_{gt}^3 + 4.0111P_{gt}^2 - 1.3682P_{gt} + 1.0342 \quad (4.2)$$

4.2.2 VARIABLE SPEED EFFICIENCY OF SYNCHRONOUS GENERATOR

As mentioned earlier, the efficiency of synchronous generator is a function of both speed and its load. For a given speed, the efficiency is approximated as a polynomial function of the load as in (4.3) and (4.4).

$$\eta_{sg} = f(\omega, P_{sg}) \quad (4.3)$$

$$\eta_{sg} = \sum_{i=0}^4 a_i P_{sg}^i \quad (4.4)$$

where the coefficients are a function of the generator speed. Figure 4.6 is the flow chart to calculate generator at any speed and load based on the efficiency curves provided by manufactures.

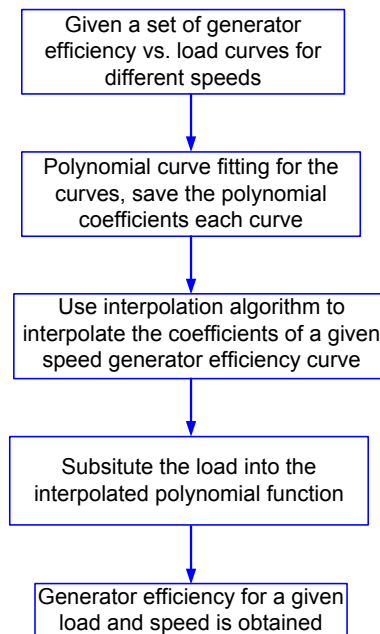


Figure 4.6 Flow chart of obtaining generator efficiency at any load and speed based on a series of efficiency curves.

4.2.3 VARIABLE SPEED EFFICIENCY OF RECTIFIERS

Figure 3.15 above shows that the efficiency of the boost type rectifiers is almost independent of the input frequency, and is a function of load only as shown in Figure 4.7 for the case of VSC. As discussed earlier, the efficiency of the rectifier can be approximated as a polynomial function of load, as shown by equation (4.5) for the three level diode clamped voltage source converter.

$$\eta_{rect} = 1.4931P_{dc}^4 + 0.777P_{dc}^3 - 0.844P_{dc}^2 + 0.4132P_{dc} + 0.8911 \quad (4.5)$$

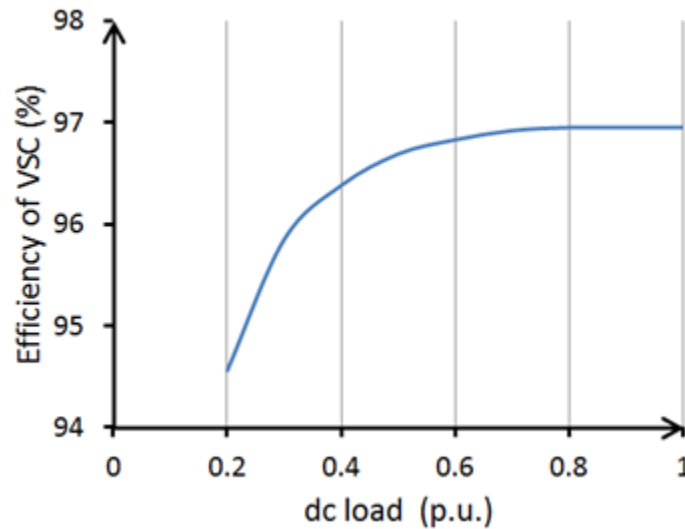


Figure 4.7 Efficiency of rectifiers vs. dc load.

4.2.4 PROCEDURE OF OBTAINING OPTIMAL SPEED REFERENCE IN MVDC POWER SYSTEM

Given and data of optimal gas turbine efficiency and its corresponding speed, generator efficiency, and the rectifier efficiency, the optimal speed of MVDC system vs. dc load is achieved by an iterative calculation process for a given load as depicted in Figure 4.8.

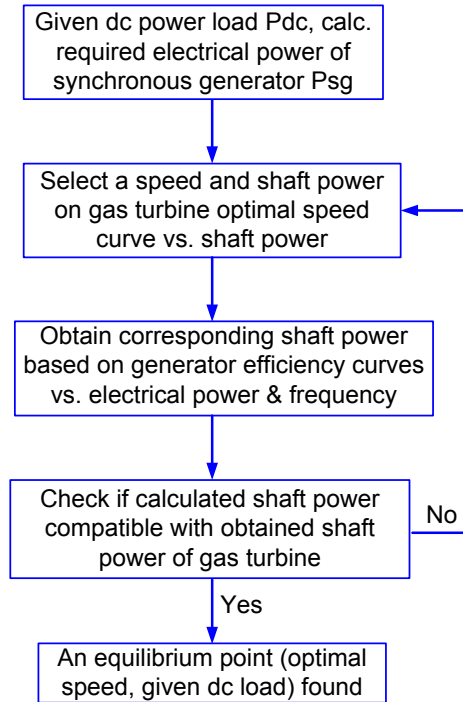


Figure 4.8 Flow chart of obtaining optimal speed reference of MVDC Power System.

4.3 RESULTS

4.3.1 STEADY-STATE EFFICINECY VS. DC LOAD

In this section results of an investigation of efficiency performance of a 25 MW MVDC power system, described in Table 4.1 in fixed speed operation and variable speed operation (VSO) are reported. Figure 4.9 shows the impact of variable speed operation on the gas turbine efficiency, generator efficiency, and rectifier (VSC) efficiency as a function of dc load, and the corresponding dc load. Figure 4.10 shows that the dc system efficiency increases as load decreases, especially for loads less than .45 p.u. the efficiency of dc system can be improved greatly by running the engine at variable speed. Figure 4.11 is the optimal speed of engine corresponding to different dc load for best efficiency.

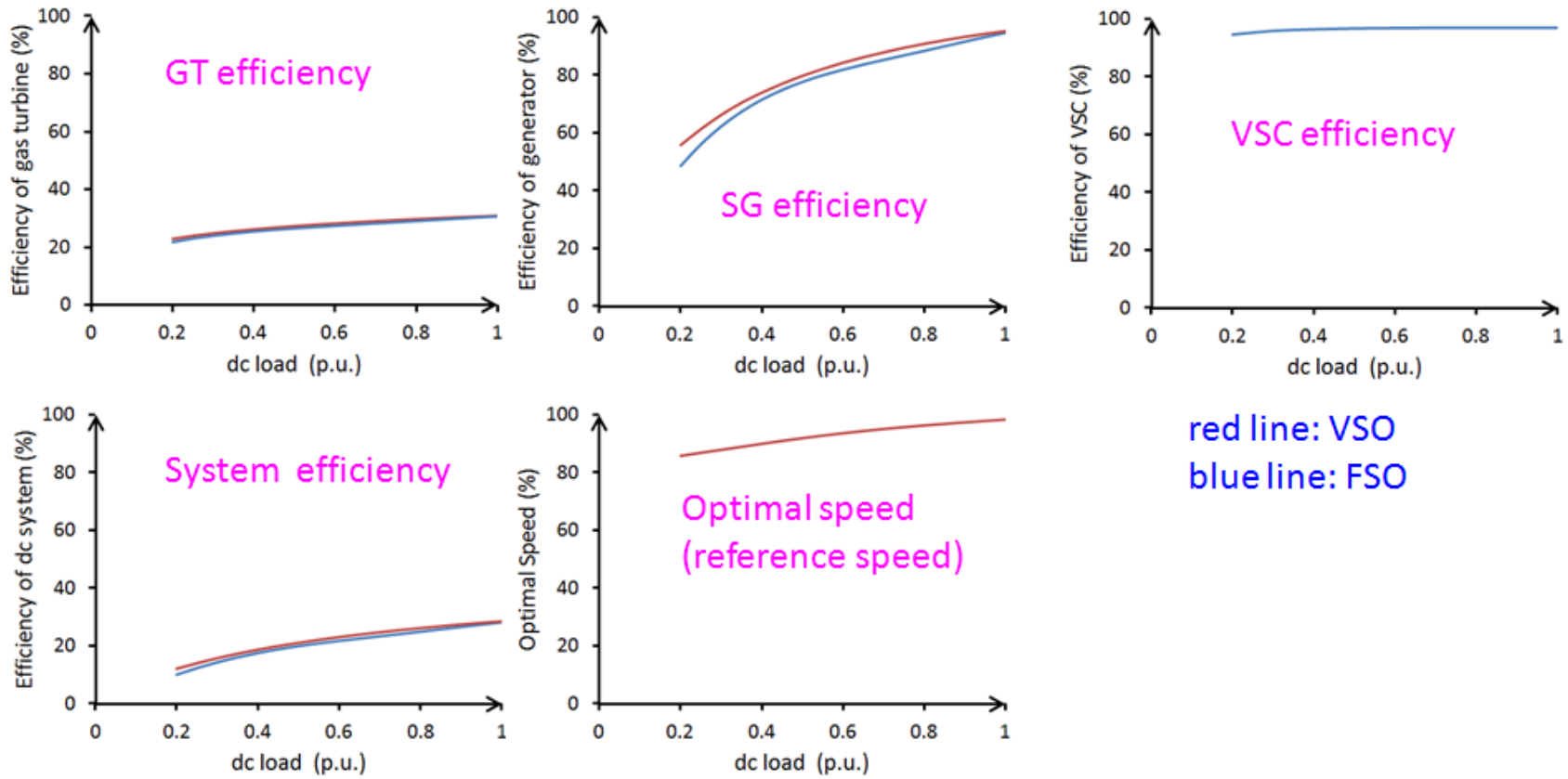


Figure 4.9 Efficiencies and optimal speed at integrated variable speed MVDC power system

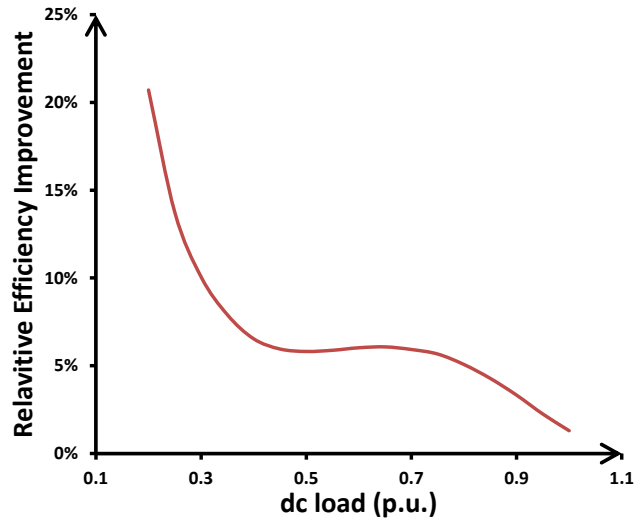


Figure 4.10 Relative efficiency improvement of dc system vs. dc load in VSO mode

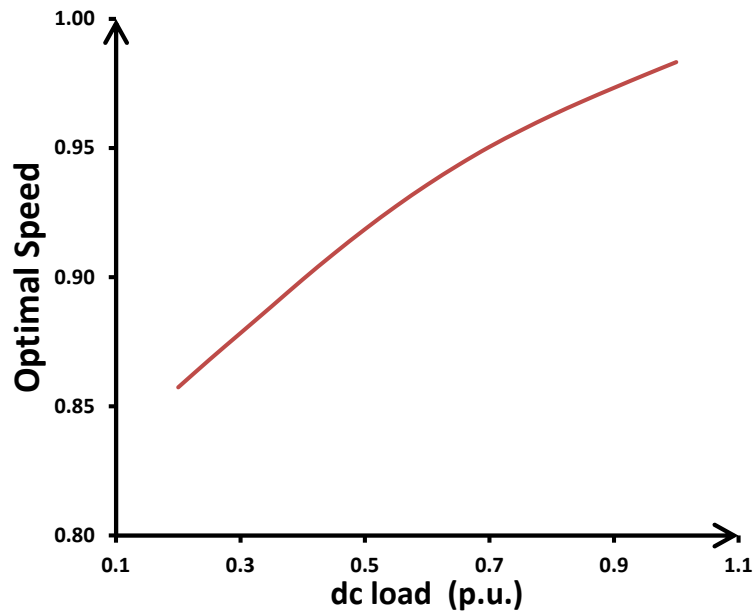


Figure 4.11 Optimal speed of variable speed MVDC Power System

4.3.2 SYSTEM DYNAMIC RESPONSE

Figure 4.12, Figure 4.13, and Figure 4.14 are the ac voltage and current, and dc bus voltage of the integrated variable speed MVDC power systems, which indicates a good steady-state performance.

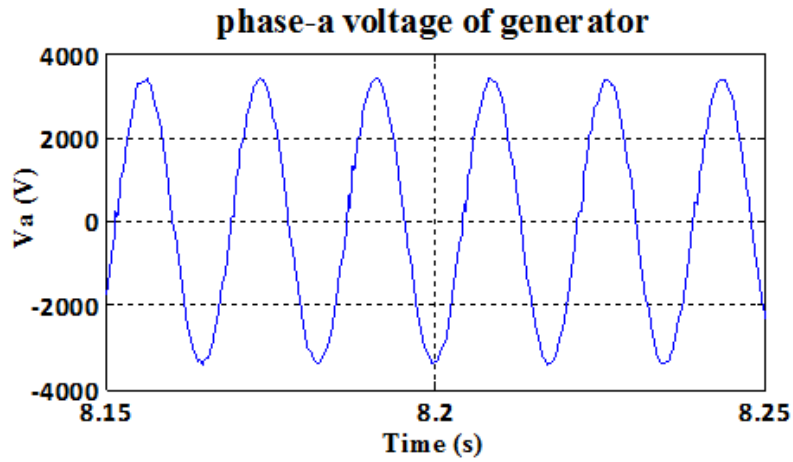


Figure 4.12 Phase-a voltage of generator

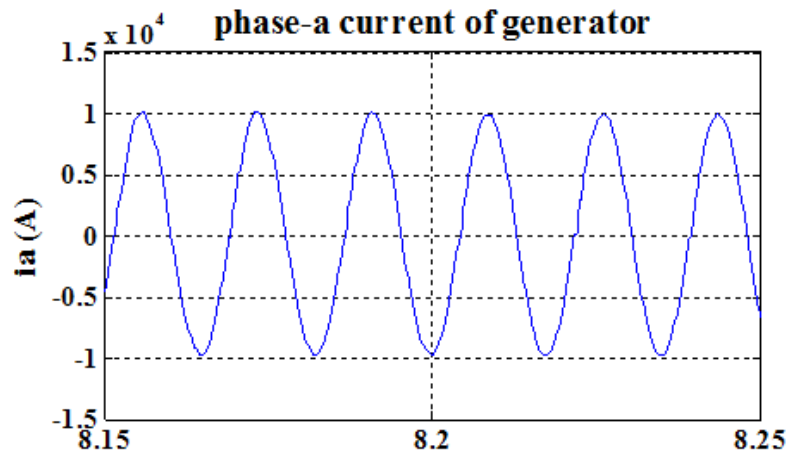


Figure 4.13 Phase-a current of generator

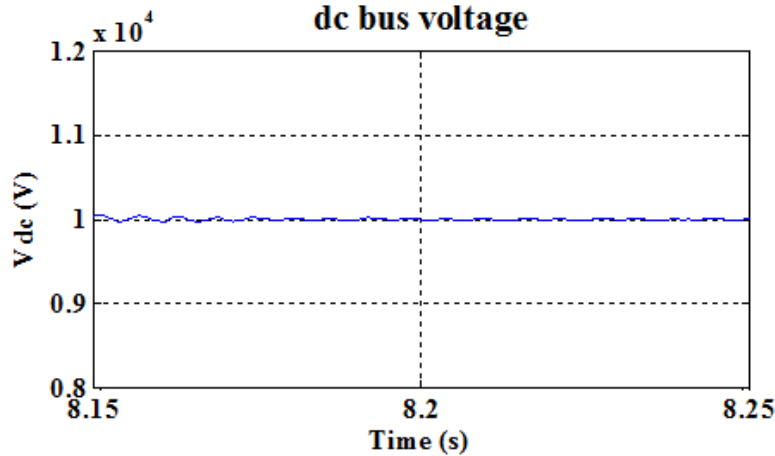


Figure 4.14 DC bus voltage

4.4 TEST ON GIVEN LOAD PROFILE

To further quantify the impact of variable speed operation of MVDC power system, a load profile that illustrates the inherent part-load characteristics of propulsion in a navy ship is used to calculate total fuel consumption for constant and variable speed operations. Figure 4.15 shows a typical speed profile of a DDG51 ship [13] (the speed profile is used as a surrogate for the electric power consumption profile on the basis that the propulsion system consumes the largest fraction of total electric power). The corresponding power profile is shown in Figure 4.9, in p.u., to illustrate the typical variation of propulsion power with ship speed. While the top speed of 30 knots requires full propulsion power, the time spent at that speed is less than 1%. This indicates that for the majority of the time, propulsion operates at part-load which will have a major impact on fuel consumption, and using variable-speed operation in this case has potential for significant fuel saving. The relationship between the efficiency η and the load power P_{dc} (p.u.) at fixed speed, as

shown in Figure 4.9, can be expressed as a polynomial equation with curve fitting as in (4.6) below:

$$\eta_{sg} = \sum_{i=0}^4 a_i P_{dc}^i \quad (4.6)$$

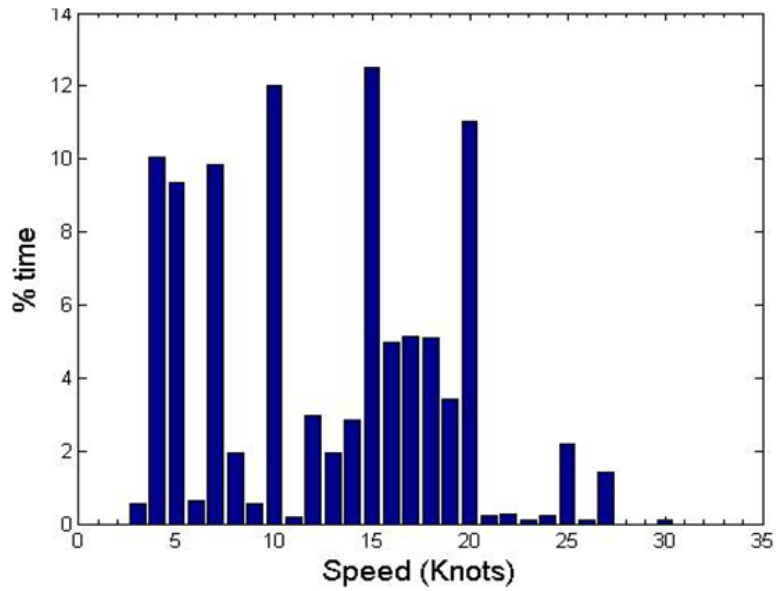


Figure 4.15 Typical propulsion speed profile of DDG-51 [13]

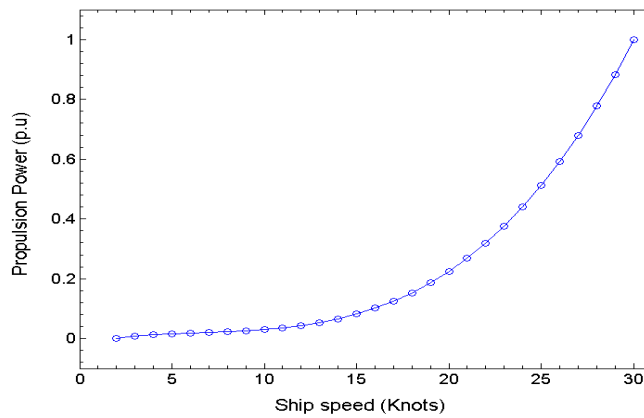


Figure 4.16 Variation of propulsion load power with ship speed

By constructing a 24-hour load profile that satisfies the speed and power profile shown in Figure 4.8 and Figure 4.9, total fuel consumption can be calculated for constant speed operation and variable speed operation of MVDC power system. For the load profile given in Figure 4.8, the total 1-day fuel consumption at variable speed and fixed speed operations for MVDC power systems are in Table 4.2. If a similar load profile was used, but with different power rating, the absolute fuel consumption reduction may be lower, but it is still 15.02% fuel consumption reduction per day as compared to original fixed speed operation. The results are summarized in Table 4.2.

Table 4.2 Example of 1- day fuel consumption for constant and variable speed operation of MVDC power systems

Operation Mode	Fuel (kg)
Fixed speed dc (N=1 p.u.)	3.25e5
Variable speed dc	2.63e5
Fuel Consumption Reduced: 23.74% (6.24e4 kg)	

It is noted that the fuel consumption reduction depends on gas turbine efficiency profile and the generator efficiency profile as a function of load and speed.

4.5 DISCUSSION AND CHAPTER SUMMARY

Previous work on variable speed operation of gas turbogenerators was extended to medium voltage dc (MVDC) power systems. Variable speed operation shows great benefit in dc system efficiency improvement. For example, when operating at 10% loading, adjusting the engine speed can improve fuel efficiency by 35% in a studied MVDC power system. Efficiency improvement increases as load decreases for the light load and high

load (less than 0.45 p.u. or more than 0.85 p.u.), the relative efficiency improvement is almost the same for medium load (between 0.45 to 0.85 p.u.), and an analysis of fuel consumption by a gas turbine that operates with a load profile representative of a typical propulsion profile for a DDG-51 ship, shows a 23.74% reduction in fuel consumption when variable speed operation is used, as compared to fixed speed operation. A procedure to control the dc power system in variable speed operation mode was developed. The procedure is based on load demand and the dynamic response of the power system was validated through modeling and simulation.

CHAPTER 5

CONCLUSION AND FUTURE WORK

5.1 CONCLUSION

This dissertation was motivated by low part-load efficiency of gas turbine and MVDC power system trends. The decoupling of speed and voltage in dc distribution system enables gas turbines to run at different speeds. However, the available gas turbine models in literature are for fixed speed operation in traditional ac power systems. In Chapter 2, the developed semi-theoretical analysis of gas turbines (both single-shaft and twin-shaft) was presented. The results from semi-theoretical analysis were also validated by modeling and simulation. To further quantify the impact of variable speed operation, an analysis of fuel consumption by a single-shaft gas turbine (operating with a load profile representative of a typical propulsion profile for a DDG-51 ship) was conducted. The fuel consumption analysis shows a 15% fuel reduction when variable speed operation is used, as compared to fixed speed operation.

In Chapter 3, an extensive comparison of boost type ac-dc rectifiers was given. The compared metrics include complexity of control strategy, number of switching devices, number/value/weight/volume of inductors and capacitors, the dc bus voltage performance (peak-peak voltage ripple, overshoot, and settling time), THD of the ac side input current and voltage, DPF, power efficiency for different load conditions, and performance under variable ac frequency operation.

Variable speed operation has great benefits in improving part-load efficiency MVDC power systems. It is implemented in the way, so that the gas turbine runs at its most efficient operating point according to the required shaft power demand. In the dc power generation chain, large amount of losses occur in the gas turbine, and running it in the most efficient way makes the dc power generation chain the most efficient. For synchronous generator, running at variable speed operation can improve efficiency, since its efficiency decreases as load decreases for fixed speed operation. However, it is noted that generator's efficiency curve as a function of speed and load is very specific to different designs. So the degree of efficiency improvement is dependent on specific generator designs. For rectifiers, i.e IGBT based rectifiers, the efficiency is almost independent of its input frequency. Therefore, variable speed operation doesn't change its efficiency characteristic much. Overall, in the dc power generation chain, variable speed operation reduces fuel consumption greatly, if the engine runs in part load often.

5.2 FUTURE WORK

In this work, the generated ac voltage from a synchronous generator is always fixed as in traditional ac power systems. Future work may take into account variable ac voltage for better dc system efficiency. Since dc power systems enables to replace wound-field synchronous generator with permanent magnet generator, this work may be extended to variable speed operation of permanent generator gas turbine driven MVDC power systems. It can also be extended to variable speed operation in multiple gas turbine driven ac or dc power systems.

REFERENCES

- [1] M. P. Boyce, *Gas Turbine Engineering Handbook*, 3rd edition. Gulf Professional Publishing, 2006.
- [2] T. Giampaolo, *Gas Turbine Handbook Principles and Practices*, 3rd edition. Fairmont Press, 2006.
- [3] J. H. Horlock, "Aero-engine derivative gas turbines for power generations: thermodynamic and economic perspectives," *ASME Journal of Engineering for Gas Turbines and Power*, vol. 119, pp. 119-123, 1997.
- [4] N. Zhang and R. Cai "Analytical solutions and typical characteristics of part-load performances of single-shaft gas turbine and its cogeneration," *Energy Conversion and Management*, vol. 43, pp. 1323-1337, 2002.
- [5] F. Mura, R. W. De Doncker, B. Persigehl, P. Jeschke and K. Hameyer, "Analysis of a gearless medium-voltage variable speed gas turbine," *VGB PowerTech*, vol. 91, No. 4, pp. 39-43, 2011.
- [6] S. K. Yee, J. Milanovic and F. M. Hughes, "Overview and comparative analysis of gas turbine models for system stability studies," *IEEE Transactions on Power Systems*, vol. 23, No. 1, pp. 108-118, Feb. 2008.
- [7] L. N. Hannett, G. Jee and B Fardanesh, "A governor/turbine model for a twin-shaft combustion turbine," *IEEE Transactions on Power Systems*, vol. 10, No. 1, pp. 133-140, Feb. 1995.
- [8] L. N. Hannett and A. Khan, "Combustion turbine dynamic model validation from tests," *IEEE Transactions on Power Systems*, vol. 8, No. 1, pp. 152-158, Feb. 1993.
- [9] W. I. Rowen, "Simplified mathematical representations of heavy-duty gas turbines," *ASME Journal of Engineering for Power*, vol. 105, pp. 865-869, Oct. 1983.
- [10] P. Pourbeik and F. Modau, "Model development and field testing of a heavy-duty gas-turbine generator," *IEEE Transactions on Power Systems*, vol. 23, No. 2, pp. 664-672, May 2008.

- [11] A. Lazzaretto and A. Toffolo, "Analytical and neural network models for gas turbine design and off-design simulation," *Int. J. Applied Thermodynamics*, vol. 4, No. 4, pp. 173-182, Dec. 2001.
- [12] Gas Turb, <http://www.gasturb.de/>
- [13] S. Z. Vijlee, A. Ouroua, L. N. Domaschk and J. H. Beno, "Directly coupled gas turbine permanent magnet generator sets for prime power generation on board electric ships," *Electric Ship Technologies Symposium, 2007, ESTS '07, IEEE*, pp. 340-347, May 2007.
- [14] H. Cohen, G. F. C. Rogers and H. I. H Saravanamuttoo, *Gas Turbine Theory*, 4th edition. Addison-Wesley, 1996.
- [15] J. H. kim, T. S. Kim, J. L. Sohn and S. T. Ro, "Comparative analysis of off-design performance characteristics of single and two shaft industrial gas turbines," *Proceedings of ASME Turbo Expo, 2002*.
- [16] Cigre Task Force C4.02.25, *Modeling of Gas turbines and Steam Turbines in Combined Cycle Power Plants*, 2003.
- [17] J. H. Horlock, *Combined Power Plants Including Combined Cycle Gas Turbines (CCGT) Plants*. New York: Pergamon, 1992.
- [18] G. Crosa, F. Pittaluga, A. Trucco, F. Beltrami, A. Torelli and F. Traverso, "Heavy-duty gas turbine plant aerothermodynamic simulation using simulink," *ASME Journal of Engineering for Gas Turbines and Power*, vol. 120, pp. 550-556, 1998.
- [19] M. T. Schobeiri, M. Attia and C. Lippke, "GETRAN: A generic, modularly structured computer code for simulation of dynamic behavior of aero- and power generation gas turbine engines," *ASME Journal of Engineering for Gas Turbines and Power*, vol. 116, pp. 483-494, 1994.
- [20] J. H. Kim, T. W. Song, T. S. Kim and S. T. Ro, "Model development and simulation of transient behavior of heavy duty gas turbines," *ASME Journal of Engineering for Gas Turbines and Power*, vol. 123, pp. 589-594, 2001.
- [21] O. O. Badmus, K. M. Eveker and C. N. Nett, "Control-oriented high frequency turbomachinery modeling: general one dimensional model development," *ASME Journal of Turbomachinery*, vol. 117, pp. 320-335, 1995.
- [22] Working Group on Prime Mover and Energy Supply Models, "Dynamic models for combined cycle plants in power system studies," *IEEE Transactions on Power Systems*, vol. 9, No. 3, pp. 1698-1708, Aug. 1994.

- [23] S. Suzaki, K. Kawata, M. Sekoguchi and M. Goto, "Mathematical model for a combined cycle plant and its implementation in an analogue power system simulator," IEEE Power Engineering Society Winter Meeting, Jan. 2000.
- [24] M. Nagpal, A. Moshref, G. K. Morison and P. Kundur, "Experience with testing and modeling of gas turbines," IEEE Power Engineering Society General Meeting, Jan-Feb. 2001.
- [25] L. Pereira, J. Undrill, D. Kosterev, D. Davies and S. Patterson, "A new thermal governor modeling approach in the WECC," IEEE Transactions on Power Systems, vol. 18, No. 2, pp. 819-829, May 2003.
- [26] J. Undrill and A. Garmendia, "Modeling of combined cycle plants in grid simulation studies," IEEE Power Engineering Society General Meeting, Jan-Feb. 2001.
- [27] L. Pereira "New thermal governor model development: its impact on operation and planning studies on the Western Interconnection," IEEE Power Energy Magazine, vol. 3, No. 3, pp. 62-70, May–Jun. 2005.
- [28] L. Pereira, D. Kosterev, D. Davies and S. Patterson, "New thermal governor model selection and validation in WECC," IEEE Transactions on Power Systems, vol. 19, No. 1, pp. 517-523, Feb. 2004.
- [29] P. Pourbeik, "Modeling of combined-cycle power plants for power system studies," IEEE Power Engineering Society General Meeting, Jul. 2003.
- [30] K. Kunitomi, A. Kurita, H. Okamoto, Y. Tada, S. Ihara, P. Pourbeik and W. W. Price, "Modeling frequency dependency of gas turbine output," IEEE Power Engineering Society General Meeting, Jan-Feb. 2001.
- [31] P. Pourbeik, The Dependence of Gas Turbine Power Output on System Frequency and Ambient Conditions, Cigre 38-101, 2002.
- [32] A. Mirandola and A. Macor, "Full load and part load operation of gas turbine-steam turbine combined plant," ISEC, Vol. 8-15, 1986.
- [33] A. Traverso, L. Magistri, A. F. Massardo, "Turbomachinery for the air management and energy recovery in fuel cell gas turbine hybrid systems," Energy, Vol 35, Issue 2, pp. 764-777, Feb. 2010.
- [34] R. Roberts, J. Brouwer, F. jabbari, T. Junker and H. Ghezel-Ayagh, "Control design of an atmospheric solid oxide fuel cell/gas turbine hybrid system: variable versus fixed speed gas turbine operation," Journal of Power Sources, Vol. 161, Issue 1, pp. 484-491, Oct. 2006.

- [35] J. Kurzke, “The importance of component maps for gas turbine performance simulations,” 12th International Symposium on Transport Phenomena and Dynamics of Rotating Machinery, Hawaii, Feb. 2008.
- [36] K. George, “Power production, delivery and utilization,” EPRI, Jun. 2006.
- [37] M. Ton, B. Fortenbery and W. Tschudi, “DC power for improved data center efficiency,” Mar. 2008.
- [38] N. Doerry, “Next generation integrated power system: NGIPS technology development road map,” Nov. 2007.
- [39] B. Singh, B. N. Singh, A. Chandra, K. Al-Haddad, A. Pandey, and D. P. Kothari, “A review of three-phase improved power quality ac-dc converters,” IEEE Transactions on Industrial Electronics, vol. 51, No. 3, pp. 641-660, Jun. 2004.
- [40] A. . H. Bhat and P. Agarwal "Review three-phase power quality improvement ac/dc converters," Electric Power Systems Research, Feb. 2007.
- [41] ABB onboard dc grid breakthrough, Nov. 2001.
<http://www.maritimeandenergy.com/news-international/2011/11/abb-onboard-dc-grid-breakthrough>
- [42] A. Siebert, A. Troedson, and S. Ebner, “ac to dc power conversion now and in the future,” IEEE Transactions on Industry Applications, vol. 38, No. 4, pp. 934-940, 2002.
- [43] American National Standard Requirements for Combustion Gas Turbine Driven Cylindrical Rotor Synchronous Generators, Institute of Electrical and Electronics Engineers, Inc.
- [44] R. M. Calfo, M. B. Smith, and J. E. Tessaro, “High-speed generators for power-dense, medium-power, gas turbine power generator sets,” American Society of Naval Engineers, 2007.
- [45] R. M. Calfo, G. E. Poole, and J. E. Tessaro, “High frequency ac power system,” American Society of Naval Engineers, 2009.
- [46] IEEE P1709/Draft D1.1 Recommended Practice for 1 to 35kV Medium Voltage Dc Power Systems on Ship, Feb 2010.
- [47] IEEE Guide for the Design and Application of Power Electronics in Electrical *Power Systems on Ships*, IEEE Std. 1662. 2008.

- [48] A. P. Prasad, P. D. Ziogas and S. Manias, "An active power factor correction technique for three-phase diode rectifiers," *IEEE Power Electronics Specialists Conference* 1989.
- [49] A. Nabae, I. Takahashi, and H. Akagi, "A new neutral-point-clamped PWM inverter," *IEEE Transactions on Industrial Applications* vol. IA-17, No. 5, pp. 518-523, 1981.
- [50] M. Liserre, F. Blaabjerg and S. Hansen, "Design and control of an LCL-filter-based three-phase active rectifier," *IEEE Transactions on Industry Applications*, vol. 41, No. 5, pp. 1281-1291, 2005.
- [51] R. Marquardt, "Stromrichterschaltungen mit verteilten energiespeichern," German Patent, DE10103031A1, Jan. 2001.
- [52] A. Lesnicar, and R. Marquardt, "An innovative modular multilevel converter topology suitable for a wide power range," *IEEE Bologna Power Tech Conference*, Jun. 2003.
- [53] Q. Tu, Z. Xu, and L. Xu, "Reduced switching-frequency modulation and circulating current suppression for modular multilevel converters," *IEEE Transactions on Power Delivery*, vol. 26, No. 3, pp. 2009-2017, 2009.
- [54] G. Skibinski, and S. Breit, "Line and load friendly drive solutions for long length cable applications in electrical submersible pump applications," *Petroleum and chemical industry technical conference, fifty-first annual conference*, 2004.
- [55] K. R. Davey, H. E. Jordan, R. J. Rodriguez, and R. E. Hebner, "Generator life and power electronics," *American Society of Naval Engineers*, 2011.
- [56] D. Li, A. Ouroua, R. Dougal, and E. Thirunavukarasu, "Variable speed operation of turbogenerators to improve part-load efficiency," *IEEE Electric Ship Technologies Symposium (ESTS)*, 2013.
- [57] D. Graovac and M. Purschel, "IGBT power losses calculation using the data-sheet parameters," *Infineon application notes*, 2009.
- [58] ABB data sheet, 5SLA 3600E170300 5SYA
- [59] ABB IGBT and Diode Modules
<http://www.abb.com/product/us/9AAC30200001.aspx?country=US>
- [60] W. J. Sarjeant, I. W. Clelland, and R. A. Price, "Capacitive components for power electronics," *Proceedings of the IEEE*, vo. 89, no.6, pp.846-855, Jun. 2001.

- [61] M. Liserre, F. Blaabjerg, and A. Dell'Aquila, "Step-by-step design procedure for a grid-connected three-phase PWM voltage source converter," *International Journal of Electronics*, vo. 91, no.8, pp.445-460, 2004.
- [62] Air core inductor calculator
http://www.m0ukd.com/Calculators/air_core_inductor_calculator/
- [63] D. Li, R. Rodrigues, R. Smart, H. Ginn, and R. A. Dougal, "Comparison of possible rectifier topologies in MVDC power systems", *American Society of Naval Engineers*, 2013. (To be submitted)
- [64] A. Arce, T. Ohishi, and S. Soares, "Optimal dispatch of generating units of the Itaipu hydroelectric plant", *IEEE Transactions on Power Systems*, vo. 91, no.8, pp.445-460, 2004.
- [65] G. Lalor, A. Mullane, and M. O'Malley, "Frequency control and wind turbine technologies" *IEEE Transactions on Power Systems*, vol. 20, No. 4, pp. 1905-1913, Nov. 2005.
- [66] M. Osenga, "Generating power at any speed?" *Diesel Progress Engines & Drives*, July 1995.
- [67] R. Saidur, "A review on electrical motors energy use and energy saving," *Renewable and Sustainable Energy Reviews*, vol. 14, Issue 3, pp. 877-898, April. 2010.
- [68] HiPak IGBT Module.
- [69] R. M. Calfo, J. A. Fulmer, and J. E. Tessaro, "Generators for use in electric marine ship propulsion systems," *Power Engineering Society Summer Meeting*, vol. 1, pp. 254-259, July 2002.
- [70] <http://www.masterresource.org/2010/05/smil-density-gas-iii/>
- [71] C. Soares, *Gas Turbines: A Handbook of Air, Land and Sea Applications*, Butterworth-Heinemann 2007.
- [72] A. K. Malkogianni, A. Tournlidakis, A. L. Polyzakis, "Comparison between two-shaft simple and single-shaft recuperated brayton cycles, using different types of gaseous fuels," *Proceedings of ASME Turbo Expo*, 2010.
- [73] NET L, *The Gas Turbine Handbook*, National Energy Technology Laboratory, 2006.
- [74] <http://answers.yahoo.com/question/index?qid=20071028043050AAsiOck>

- [75] C. B. Meher-Homji, T. Hattenbach, D. Messersmith, H. P. Weyermann, K. Masani and S. Gandhi, "World's first application of aeroderivative gas turbine drivers for the conocophillips optimized cascade LNG process," Bechtel Corporation, 2008.
- [76] L. S. Langston, G. Opdyke and D. Enterprises, "Introduction to gas turbine for nonengineers," *Global Gas Turbine News*, vol. 37, No. 2, 1997.
- [77] Alstom GT24/GT26 sequential combustion gas turbine.

APPENDIX A GAS TURBINE

This section describes the background of the gas turbine modeling including the overview of gas turbine, the comparison between the single-shaft and twin-shaft gas turbine and the methods of gas turbine modeling.

A.1 GAS TURBINE OVERVIEW

As prime movers, gas turbines have been widely applied in both mechanical drive applications and electrical power generation ranging from tens of kW, such as micro-gas turbine to hundreds of MWs such as frame type heavy-duty gas turbines. Based on power ratings and applications, for simple cycle gas turbines, it might be categorized into five broad groups as in Table A.1. Compared to other type of engines, gas turbine is more preferable in terms of the consideration of weight, compactness, fast response to load changes and flexibility of fuel choices [1] [2] [70]. It has high power-to-weight ratio and runs on both liquids and gases, such as natural gas, diesel fuel, methane, crude, low-Btu gases, vaporized fuel oils, naphtha and biomass gases [1] [2] [3] [71]. Based on the characteristics above, gas turbines are largely found in utilities as peak power, remote power generation power plant, aerospace industry, marine applications to power the propulsion system, etc. In contrast to simply cycle application, the fuel efficiency of gas turbine is greatly improved when it runs in cogeneration mode or as combined cycle gas turbine. Besides, in terms of capital cost and installation time, as distributed generation

technologies, among the engines, gas turbine is the best choice for peaking power as in Table A.2 (reproduced from ref [1]) considering a deregulated utility.

Table A.1 Categories of simple cycle gas turbine

Types of Gas Turbine	Size Range	Efficiency
Frame type heavy-duty gas turbine	3 – 480 MW	30-46%
Aero-derivative gas turbine	2.5 – 50 MW	35-45%
Industrial type gas turbine	2.5 – 15 MW	
Small gas turbine	0.5 – 2.5 MW	15-25%
Micro-gas turbine	20 – 350 kW	

According to the configuration of the shafts of gas turbine, it might be categorized into single spool-integral output shaft gas turbine (also called single shaft gas turbine), single spool-split output shaft gas turbine (also called twin-shaft gas turbine) and dual spool-split output shaft gas turbine. Twin shaft gas turbine is a single-shaft gas turbine (high pressure turbine) driving a power turbine (low pressure turbine) through aerodynamic coupling. The dual spool-split output shaft gas turbine is a twin-shaft gas turbine that has independent low and high pressure compressors and turbines. Therefore, it has three shafts, low pressure compressor-turbine rotor, high pressure compressor-turbine rotor and free power turbine rotor. The sketches of the three types of gas turbine are showed in Figure A.1, Figure A.2 and Figure A.3 (directly copied from ref [2]). A complete gas turbine engine family tree is illustrated in Figure A.5 (directly copied from ref [71]).

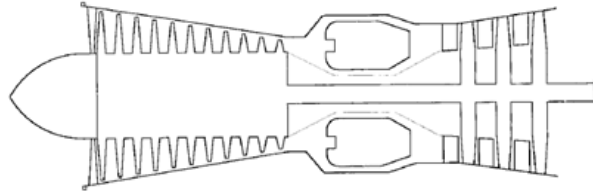


Figure A.1 This Sketch of a single shaft gas turbine [2]

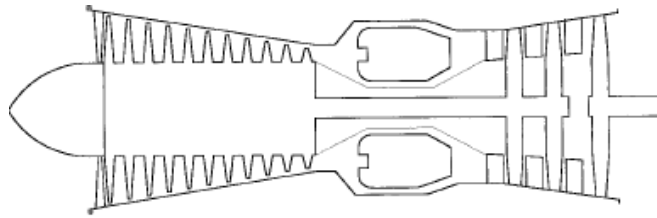


Figure A.2 Sketch of a twin-shaft gas turbine [2]

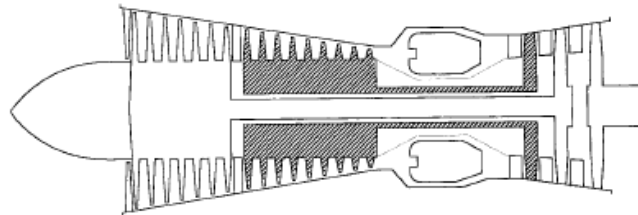


Figure A.3 Sketch of a dual spool-split output shaft gas turbine [2]

A.2 COMPARISON OVERVIEW BETWEEN SINGLE-SHAFT AND TWIN-SHAFT GAS TURBINES

As In this work, a twin-shaft gas turbine model is selected considering that the power turbine connected to the driven equipment (in electricity generation, it is a generator) can run at speeds that are different from the high pressure gas turbine speed (or called gas generator speed). So the power turbine can run at the same speed as the driven equipment

which eliminates the reduction gear box. The diagrams of a single-shaft gas turbine and a twin-shaft gas turbine are shown in Figure 2.2 and Figure 2.3. Considering the efficiency in partly load, twin-shaft gas turbine is preferred [72] [15], since the speed of compressor-high pressure turbine shaft is flexible to be adjusted to obtain the best pressure ratio which allows the least fuel.

Twin-shaft gas turbine is also considered as aero-derivative gas turbine, which is based on aircraft engine. Since the air-craft engine places more concerns on weight, volume and not that long continuous operation, the twin-shaft gas turbine is lighter and more expensive, has modular construction, and requires more maintenance. [73] [71] [74] [75] [76] give details about the difference between sing-shaft and twin-shaft gas turbine engines.

A.3 GAS TURBINE EFFICIENCY

The efficiency of gas turbine is relatively low compared to other types of engines since almost one thirds of power is consumed by the compressor itself in the gas turbine engine. There are a couple of ways to improve the efficiency of gas turbine including increasing the firing temperature, combining with steam turbine to use the exhaust waste of the gas turbine, increasing the compressor pressure, etc. [71] [77]. Not only, the efficiency at design load is low, the part-load efficiency is even lower. Figure A.4 (directly copied from ref [14]) is the equilibrium running line of a single-shaft gas turbine driving different loads, where the efficiency of driving a generator is decreasing dramatically for part-load condition.

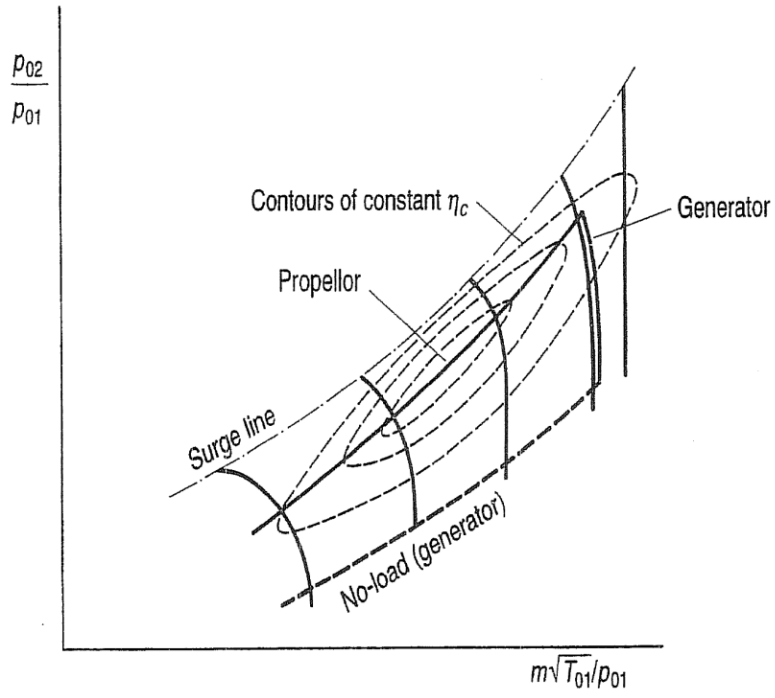


Figure A.4 Equilibrium running line of compressor

Table A.2 Economic and operation characteristics of plant [1]

Type of Plant	Capital Cost \$/kW	Heat Rate Btu/kWh kJ/kWh	Net Efficiency	Variable Operation & Maintenance (\$/MWh)	Fixed Operation & Maintenance (\$/MWh)	Availability	Reliability	Time from Planning to Completion Months
Simple cycle gas turbine (2500°F/1371°C)	300-350	7528-8000	45	5.8	0.23	88 – 95%	97 – 99%	10 – 12
Simple cycle gas turbine oil fired	400-500	8322-8229	41	6.2	0.25	85 – 90%	95 – 97%	12 – 16
Simple cycle gas turbine crude fired	500-600	10662-11250	32	13.5	0.25	75 – 80%	90 – 95%	12 – 16
Regenerative gas turbine natural gas fired	375-575	6824 -7200	50	6.0	0.25	86 – 93%	96 – 98%	12 – 16
Combined cycle gas turbine	600-900	6203-6545	55	4.0	0.35	84 – 90%	95 – 98%	22 – 24
Advanced gas turbine combined cycle power plant	800-1000	5249-5538	65	4.5	0.4	75 – 85%	94 – 96%	28 – 30
Combined cycle coal gasification	1200-1400	6950-7332	49	7.0	1.45	75 – 85%	90 – 95%	30 – 36
Combined cycle fluidized bed	1200-1400	7300-7701	47	7.0	1.45	75 – 85%	90 – 95%	30 – 36
Nuclear power	1800-200	10000-10550	47	7.0	2.28	80 – 89%	92 – 98%	48 – 60
Steam plant coal fired	800-1000	9749-10285	34	8	1.43	82 – 89%	94 – 97%	36 – 42
Diesel generator-diesel fired	400-500	7582-8000	35	3	4.7	90 – 95%	96 – 98%	12 – 16
Diesel generator-power plant oil fired	600-700	8124-8570	45	6.2	4.7	85 – 90%	92 – 95%	16 – 18
Gas engine generator power plant	650-750	7300-7701	42	7.2	4.7	92 – 96%	96 – 98%	12 – 16

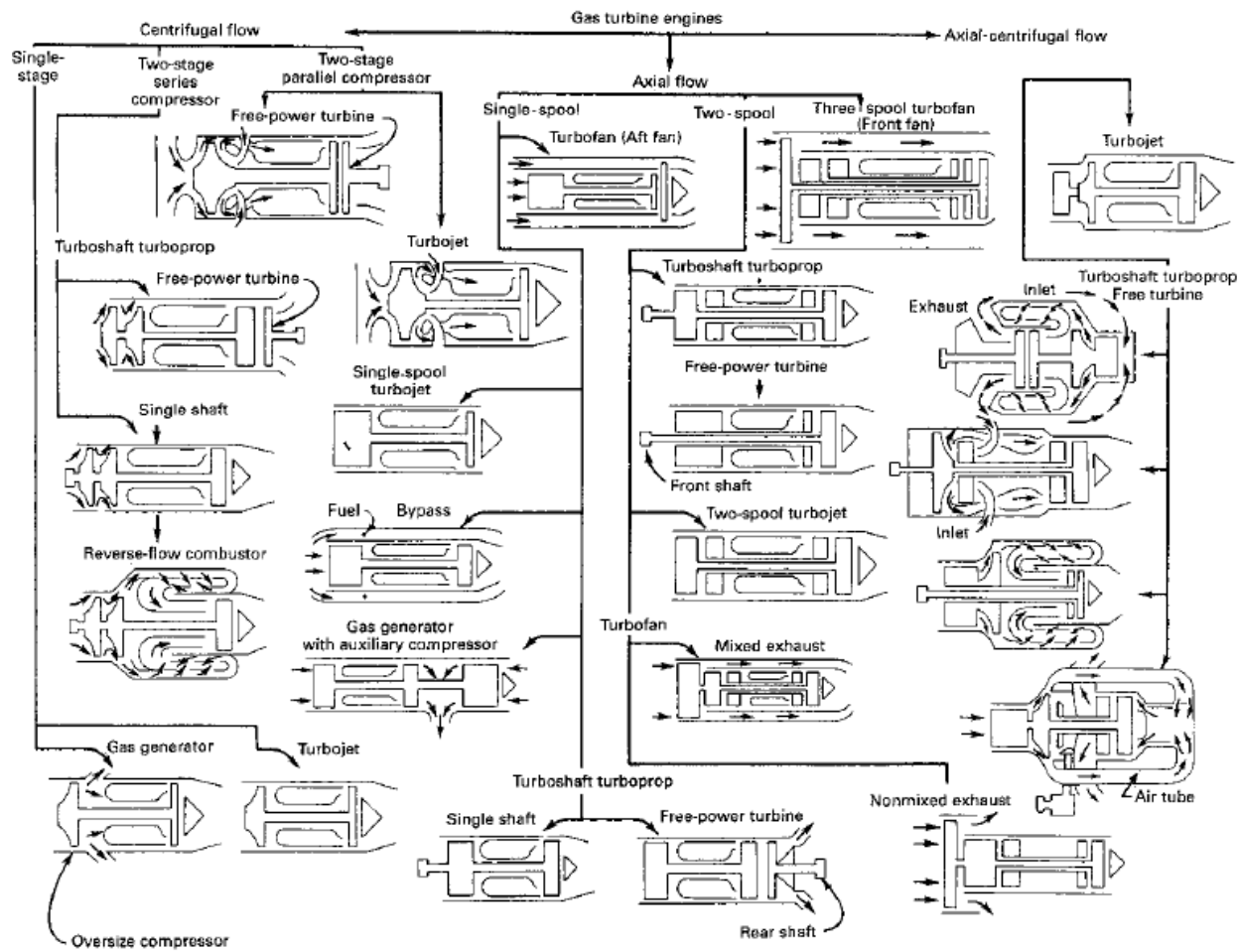


Figure A.5 Gas turbine family tree [71]